



12-2013

BUDGET-CONSTRAINED POWER SYSTEM RELIABILITY OPTIMIZATION

Robert Jonathan Mosteller
University of Tennessee - Knoxville, rmostell@utk.edu

Follow this and additional works at: https://trace.tennessee.edu/utk_gradthes

Recommended Citation

Mosteller, Robert Jonathan, "BUDGET-CONSTRAINED POWER SYSTEM RELIABILITY OPTIMIZATION. " Master's Thesis, University of Tennessee, 2013.
https://trace.tennessee.edu/utk_gradthes/2627

This Thesis is brought to you for free and open access by the Graduate School at TRACE: Tennessee Research and Creative Exchange. It has been accepted for inclusion in Masters Theses by an authorized administrator of TRACE: Tennessee Research and Creative Exchange. For more information, please contact trace@utk.edu.

To the Graduate Council:

I am submitting herewith a thesis written by Robert Jonathan Mosteller entitled "BUDGET-CONSTRAINED POWER SYSTEM RELIABILITY OPTIMIZATION." I have examined the final electronic copy of this thesis for form and content and recommend that it be accepted in partial fulfillment of the requirements for the degree of Master of Science, with a major in Reliability and Maintainability Engineering.

James Ostrowski, Major Professor

We have read this thesis and recommend its acceptance:

Mingzhou Jin, Jamie B. Coble

Accepted for the Council:

Carolyn R. Hodges

Vice Provost and Dean of the Graduate School

(Original signatures are on file with official student records.)

BUDGET-CONSTRAINED POWER SYSTEM RELIABILITY OPTIMIZATION

A Thesis Presented for the
Master of Science
Degree
The University of Tennessee, Knoxville

Robert Jonathan Mosteller

December 2013

Copyright © 2013 by Robert J. Mosteller
All rights reserved.

DEDICATION

To Christian, Caroline & Jack.

Jack, you will always be my sweet boy.

Caroline, you are an extraordinarily intelligent and beautiful girl. Your mom and I will always be proud of you. Call Jack for directions.

Christian, you are the kindest person I've ever known. Together we make the best team.

I love you all and promise graduate school won't be replaced (again) with Ironman races.
Until next semester and the next swim buoy...

ACKNOWLEDGEMENTS

This thesis started as an optimization problem using the cutting-stock algorithm applied to underground power cable pulling to minimize scrap and reel carrier movements.

It then morphed into a study of power component lifetime modeling and the reliability impacts of various levels of equipment replacement. Some spatial load forecasting using various regression models was going to be done for good measure.

Circuit breaker operational failures called, but things still didn't feel quite right.

After years of tortuous capital budgeting cycles, the work finally coalesced into its proper form.

Through all of its iterations, Dr. Jim Ostrowski patiently offered advice and guidance.

Thank you.

ABSTRACT

Electric utilities face constant pressure from regulators to defer rate increases while simultaneously maintaining or improving levels of service. Capital spending projects are coming under increasing scrutiny as the costs of the projects can no longer be assumed to be rolled into projected rate increases. At the same time, utility customers expect near uninterrupted service to their homes and businesses. Electric lines and components that make up the power system are getting older and are reaching or have exceeded an assumed end-of-life.

Planners at these utilities need a way to prioritize constrained budget dollars across seemingly disparate transmission, substation, and distribution work areas. This thesis provides a framework for quantifying the reliability impacts of these different projects as measured by Customer-Minutes of Interruption (CMI) avoided. Transmission lines are modeled as continuous time Markov processes with common-cause failure modes. The parallel-series configuration of the substation and failure modes of its components is evaluated using Failure Mode and Effects Analysis (FMEA). Circuit breaker operational failures are evaluated and Poisson process models are fitted by interrupting medium. The transmission and substation systems are then evaluated as a decoupled equivalent source per feeder in series with the distribution system. Competing projects impacts are evaluated and prioritized based upon dollars spent per CMI avoided (\$/CMI).

TABLE OF CONTENTS

Chapter 1 Introduction	1
1.1 Power System Overview	1
1.1.1 Transmission Subsystem Overview	3
1.1.2 Substation Subsystem Overview	3
1.1.3 Distribution Subsystem Overview	5
1.2 Thesis Goals and Approach	6
1.3 Thesis Outline	8
Chapter 2 Literature Review Of Power System Reliability Evaluation	10
2.1 Reliability and Reliability Cost Evaluation	10
2.1.1 Power Industry Standards.....	10
2.1.2 Minimization of Societal Costs	12
2.1.3 Benefits & Drawbacks of Each Method.....	16
2.2 System Reliability Evaluation.....	17
2.2.1 Discrete Markov Chains	17
2.2.2 Continuous Markov Processes	22
2.2.3 Series Systems	26
2.2.4 Parallel Systems	28
2.2.5 Combined Series-Parallel Systems.....	29
2.3 Transmission System Assessment	32
2.4 Substation System Assessment	35
2.4.1 Active and Passive Failures	36
2.4.2 Circuit Breaker Operational Failure Modeling	38
2.4.3 Substation Failure Mode and Effects Analysis	46
2.5 Distribution System Assessment.....	48
2.6 Decoupled Composite Model Assessment.....	51
2.7 Reliability Benefit-Cost Analysis	51
Chapter 3 Composite Power System Reliability Evaluation	53
3.1 Transmission Reliability Evaluation	53
3.2 Substation Reliability Evaluation	57
3.2.1 Substation Model.....	57
3.2.2 Circuit Breaker Operational Failure Recurrence Analysis	59
3.2.3 Substation Component Modeling.....	68
3.2.4 Substation Reliability Evaluation	69
3.2.5 Distribution Reliability Assessment.....	72
3.3 Composite Reliability Evaluation	76
Chapter 4 Budget-Constrained Power System Reliability Optimization.....	78
4.1 Case Studies and Evaluation	78
4.1.1 Base Case	78
4.1.2 Case 1: Install Automated Switches by Feeder	78
4.1.3 Case 2: Replace Feeder Breakers by Feeder	79
4.1.4 Case 3: Replace 3-Ø Underground Getaway Cable by Feeder	80
4.1.5 Case 4: Replace 1-Ø Underground Residential Distribution Cable by Feeder ...	81

4.1.6 Case 5: 161 kV Transmission Improvements.....	83
4.2 Budget-Constrained Project Optimization.....	85
4.2.1 Case 1 (Install Automated Switches) Reliability Benefit-Cost Analysis.....	85
4.2.2 Case 2 (Feeder Breaker Replacement) Reliability Benefit-Cost Analysis.....	87
4.2.3 Case 3 (3-Ø Getaway Cable Replacement) Reliability Benefit-Cost Analysis...	88
4.2.4 Case 4 (1-Ø URD Cable Replacement) Reliability Benefit-Cost Analysis	89
4.2.5 Case 5 Reliability Benefit-Cost Analysis.....	89
4.2.6 Budget Constrained Reliability Optimization	90
Chapter 5 Conclusions and Recommendations.....	93
5.1 Conclusions.....	93
5.2 Future Work	93
List Of References	94
Vita.....	97

LIST OF TABLES

Table 2.1 State Probabilities	19
Table 2.2 System Reliability of Figure 2.9 using FMEA	32
Table 2.3 Example MCF Calculation	43
Table 2.4 Component Data for Substation in Figure 2.11	47
Table 2.5 System Reliability of Load Point A in Figure 2.11	48
Table 3.1 Transmission Circuit Lengths	54
Table 3.2 Transmission Line Data	55
Table 3.3 MLE Fitted NHPP Model Parameters	66
Table 3.4 Substation Component Modeling	68
Table 3.5 Feeder #1 Equivalent Source	69
Table 3.6 Feeder #2 Equivalent Source	70
Table 3.7 Feeder #3 Equivalent Source	71
Table 3.8 Feeder #4 Equivalent Source	72
Table 3.9 Distribution Section Lengths	73
Table 3.10 Load Point Customer Information	73
Table 3.11 Distribution Component Data	74
Table 3.12 Load Point Reliability Results	76
Table 3.13 Base Case Reliability Results	77
Table 4.1 Switching Component Information	79
Table 4.2 Case 1 Reliability Results	79
Table 4.3 Feeder Breaker Component Information	80
Table 4.4 Case 2 Reliability Results	80
Table 4.5 3-Ø Getaway Cable Component Information	81
Table 4.6 Case 3 Reliability Results	81
Table 4.7 1-Ø URD Cable Component Information	82
Table 4.8 Case 4 Reliability Results	82
Table 4.9 Proposed Transmission Circuit Lengths	84
Table 4.10 Case 5 Reliability Results	85
Table 4.11 Case 1 Reliability Improvements & Project Costs	86
Table 4.12 Case 1 Reliability Benefit-Cost Analysis	86
Table 4.13 Case 2 Reliability Improvements & Project Costs	87
Table 4.14 Case 2 Reliability Benefit-Cost Analysis	87
Table 4.15 Case 3 Reliability Improvements & Project Costs	88
Table 4.16 Case 3 Reliability Benefit-Cost Analysis	88
Table 4.17 Case 4 Reliability Improvements & Project Costs	89
Table 4.18 Case 4 Reliability Benefit-Cost Analysis	89
Table 4.19 Case 5 Reliability Improvements	90
Table 4.20 Case 5 Reliability Benefit-Cost Analysis	90
Table 4.21 CMI-Optimized Global Solution For Power System	91

LIST OF FIGURES

Figure 1.1 Traditional Power System	2
Figure 1.2 Substation One Line Diagram and Elevation	4
Figure 1.3 Typical Distribution System.....	6
Figure 2.1 Total Societal Costs	12
Figure 2.2 Two State System	17
Figure 2.3 Tree Diagram.....	18
Figure 2.4 Steady-State Probabilities.....	19
Figure 2.5 Two-State Continuous Model.....	23
Figure 2.6 Two Component Repairable System	24
Figure 2.7 Equivalent Series System	26
Figure 2.8 Equivalent Parallel System.....	28
Figure 2.9 Combined Series-Parallel System	31
Figure 2.10 State Space Diagram w/Common Cause Failures	33
Figure 2.11 Simplified One-Line Diagram of Figure 1.2 Substation	35
Figure 2.12 Three-State Component Model	36
Figure 2.13 Two-State Component Model	37
Figure 2.14 Equivalent Component Model.....	37
Figure 2.15 Constant Rate of Occurrence of Failure (ROCOF)	40
Figure 2.16 Increasing ROCOF	40
Figure 2.17 Decreasing ROCOF.....	40
Figure 2.18 Sample Mean Cumulative Function (MCF)	41
Figure 2.19 Example Event Plot	43
Figure 2.20 Example MCF	43
Figure 2.21 Feeder #1	50
Figure 3.1 Existing Transmission Route.....	54
Figure 3.2 State 4 Probabilities for Substation Transmission Feed	56
Figure 3.3 Substation One-Line Diagram.....	58
Figure 3.4 Feeder Breakers In Service.....	60
Figure 3.5 Feeder Breakers by Age	60
Figure 3.6 Breaker Event Plot by Calendar	61
Figure 3.7 Shifted Breaker Event Plot	61
Figure 3.8 Failure Modes	62
Figure 3.9 Pooled MCF.....	63
Figure 3.10 Non-Parametric Oil MCF	64
Figure 3.11 Non-Parametric Gas MCF	64
Figure 3.12 Non-Parametric Vacuum MCF.....	64
Figure 3.13 Gas vs. Vacuum Breakers.....	65
Figure 3.14 Fitted Oil MCF	67
Figure 3.15 Fitted Gas MCF	67
Figure 3.16 Fitted Vacuum MCF.....	67
Figure 3.17 Recurrence Rates	67
Figure 3.18 Distribution System	75

Figure 4.1 Proposed Transmission Improvements.....	83
Figure 4.2 State 4 Probabilities for Transmission Lines.....	84
Figure 4.3 Cumulative Budget Per CMI Purchased.....	92

LIST OF ATTACHMENTS

File 1 Customer Damage Function Coefficients (Excel file).....	cdf_coefficients.xls
File 2 Feeder Breaker Failure Data (Excel file).....	feeder_summary.xls
File 3 Pooled Feeder Breaker MCF & Failure Prediction (Excel file).....	system_mcf.xls
File 4 Oil Breaker MCF & Failure Prediction (Excel file).....	oil_mcf.xls
File 5 Gas Breaker MCF & Failure Prediction (Excel file).....	gas_mcf.xls
File 6 Vacuum Breaker MCF & Failure Prediction (Excel file).....	vacuum_mcf.xls

CHAPTER 1

INTRODUCTION

1.1 Power System Overview

The electric power grid has been described as the most complicated machine on Earth. Conceptually it is very simple; an illustration of a traditional system is provided in Figure 1.1 (Brown, 2009). Power is traditionally generated at large coal- or natural gas-fired, hydroelectric, or nuclear generating stations generally remotely located from population centers. The voltage is then stepped up at generation substations to a voltage suitable for long distance transmission. Large steel towers support high voltage transmission circuits emanating from these generation substations and span miles to large transmission substations. The transmission substations allow for reconfiguration and/or voltage transformation.

Transmission towers then connect the transmission substations, via what is sometimes referred to as subtransmission circuits, to distribution substations located closer to the loads serviced where the voltage is stepped back down to what is generally referred to as “primary” distribution voltage. Feeder circuits on wood poles or underground cables branch out from the distribution substations to the customer where distribution transformers step the voltage down to “secondary” distribution voltage appropriate for use by the customer.

This thesis will focus only on the transmission feeds to the distribution substation, the distribution substation itself, and the primary distribution system. It is assumed that the sources feeding the transmission system are perfectly reliable. These transmission, substation, and distribution subsystems will be introduced a bit further in forthcoming sections.

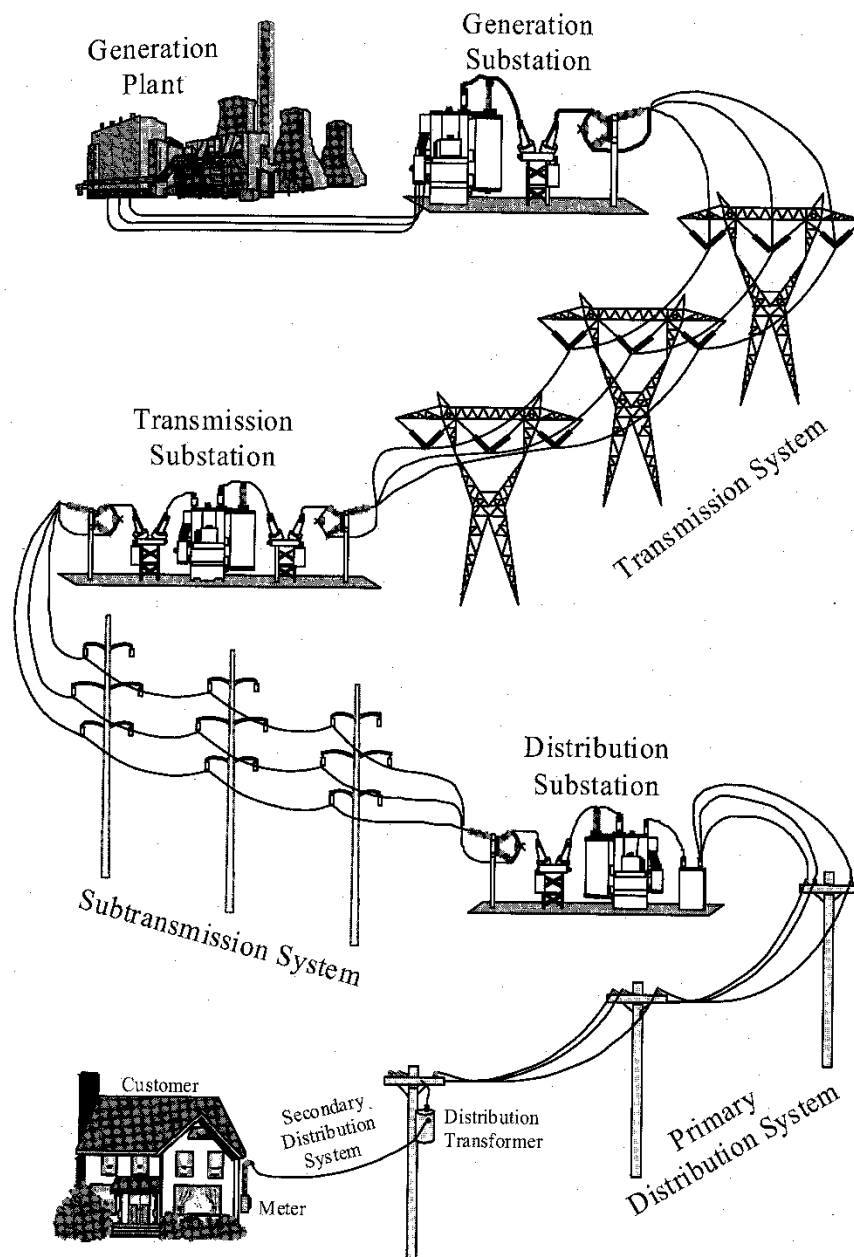


Figure 1.1 Traditional Power System

1.1.1 Transmission Subsystem Overview

The purpose of the transmission system is to connect far flung generation facilities to load centers. In most cases, lattice steel towers or tubular steel poles support transmission circuits over long distances, although underground transmission circuits (HPFF, HPGF, extruded EPR or XLPE dielectric) do exist, generally in urban centers and span much shorter distances due to the significant installation cost. The voltage level (phase-to-phase voltages will be used throughout) is very high – typical voltage levels in the United States include 69 kV, 115 kV, 138 kV, 161 kV, 230 kV, 345 kV, 500 kV, 765 kV, and 1100 kV (Brown 2009).

Transmission circuits terminate at switching stations, transmission substations, or distribution substations. Transmission switching stations allow for transmission circuits to be reconfigured and generally increase operational flexibility. Transmission substations step down the voltage from one transmission voltage to another. For example, a 500 kV Tennessee Valley Authority (TVA) transmission line is stepped down to 161 kV at a TVA distributor's transmission substation, which would be located closer to the loads serviced. Distribution substations generally have two transmission feeds for improved reliability. These distribution substations will be explored further in the next section.

1.1.2 Substation Subsystem Overview

The main purpose of the distribution substation is to transform the voltage from transmission levels to primary distribution levels, generally from 12 to 35 kV. It also allows for some feeder reconfiguration in the event of some anomaly. Figure 1.2 shows an example of a very simple substation one-line diagram and elevation. This is a 161-23 kV single transformer bank, three feeder substation with a T-tapped transmission feed. The incoming 161 kV transmission line feeds through a disconnect switch which cannot break load but is meant to isolate and serve as a visual confirmation of open circuit. The high voltage circuit breaker is meant to break under load for protection.

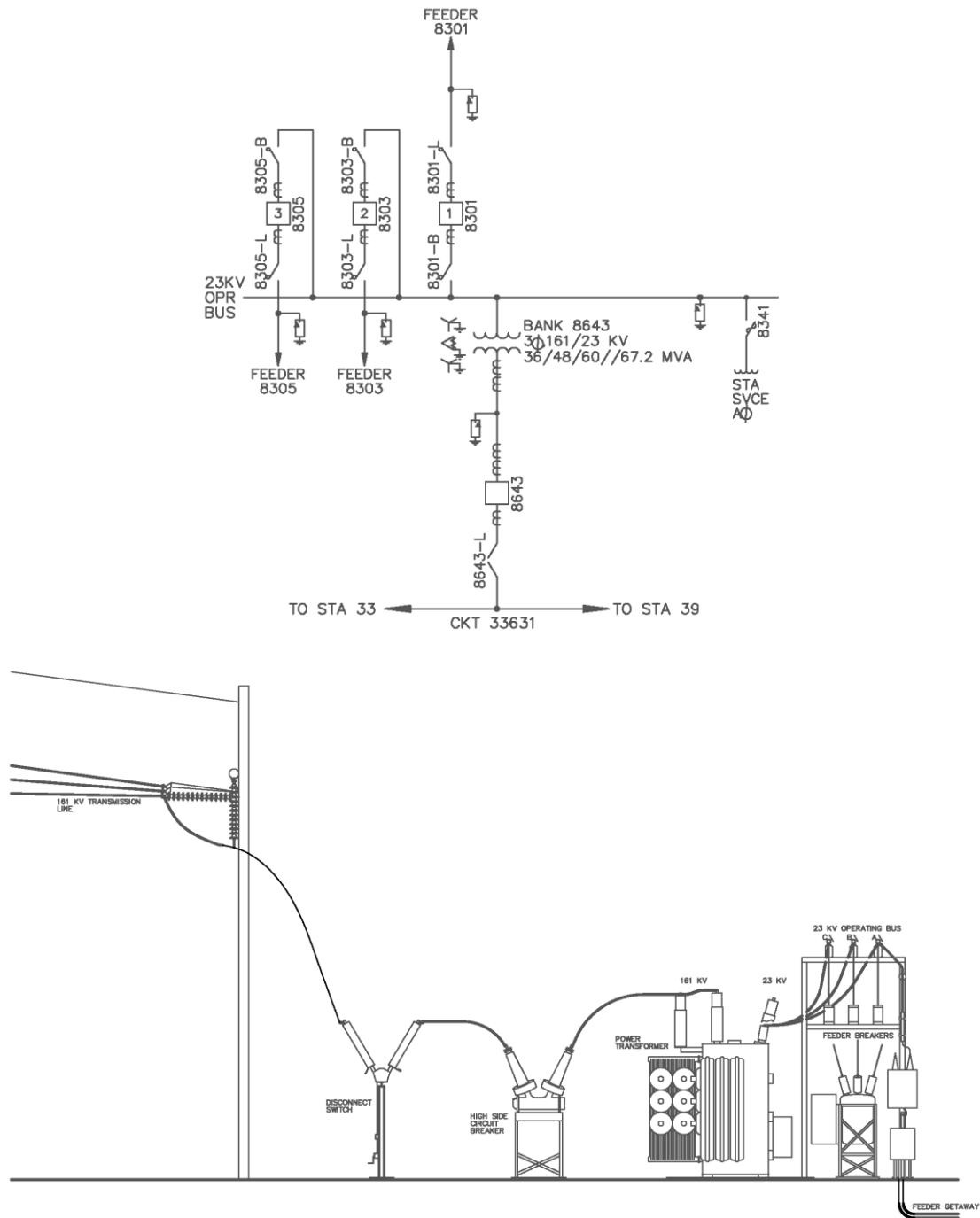


Figure 1.2 Substation One Line Diagram and Elevation

The power transformer steps the voltage down from 161 kV to 23 kV and feeds a common 23 kV operating bus. Tapped off of this bus are the three feeder breakers with non-load break disconnect switches on both the source and load sides. The feeder breakers are meant to protect the substation in the event of faults on the distribution side. Feeder getaways, generally underground or sometimes overhead, radiate out from the substation to begin the distribution system.

This particular arrangement is particularly susceptible to reliability problems in that the components are arranged in series. The failure of any single component will result in loss of service for all customers fed from this substation. It has been estimated that approximately 20% of customer interruptions originate at the substation and transmission level (Billinton & Jonnavitihula, 1996). Although the example in Figure 1.2 is an actual substation in operation in the Southeastern U.S., most substation arrangements (including the model to be used in this thesis) have a much more involved parallel/series configuration with looped transmission feeds. This allows for more flexible and reliable operation at the expense of higher cost.

1.1.3 Distribution Subsystem Overview

The distribution system connects the distribution substation with the distribution transformers, which then provide service to the customer at the service entrance. Figure 1.3, taken from Brown (2009), shows an example four feeder distribution system. Generally, the feeders get away from the substation underground in concrete-encased duct banks and rise up to start the main backbone feeder overhead on wood poles. Fused lateral taps, either 1-Ø, 2-Ø, or 3-Ø, branch off of the backbone feeder to distribution transformers. Normally closed sectionalizing switches allow for sectionalization along the length of the backbone; normally open switches between adjacent feeders allow for load transfer. In traditional distribution systems, these switches are operated manually. With the advent of Distributed Automation (DA) technologies, components including these switches are able to be operated remotely by operators thereby reducing response times.

The distribution system in Figure 1.3 represents a typical scenario, though it should be noted that there are many other options available. The same can be said of the system design on the secondary side of the distribution transformer, particularly in regards to secondary networks, but these secondary arrangements will not be addressed further in this work.

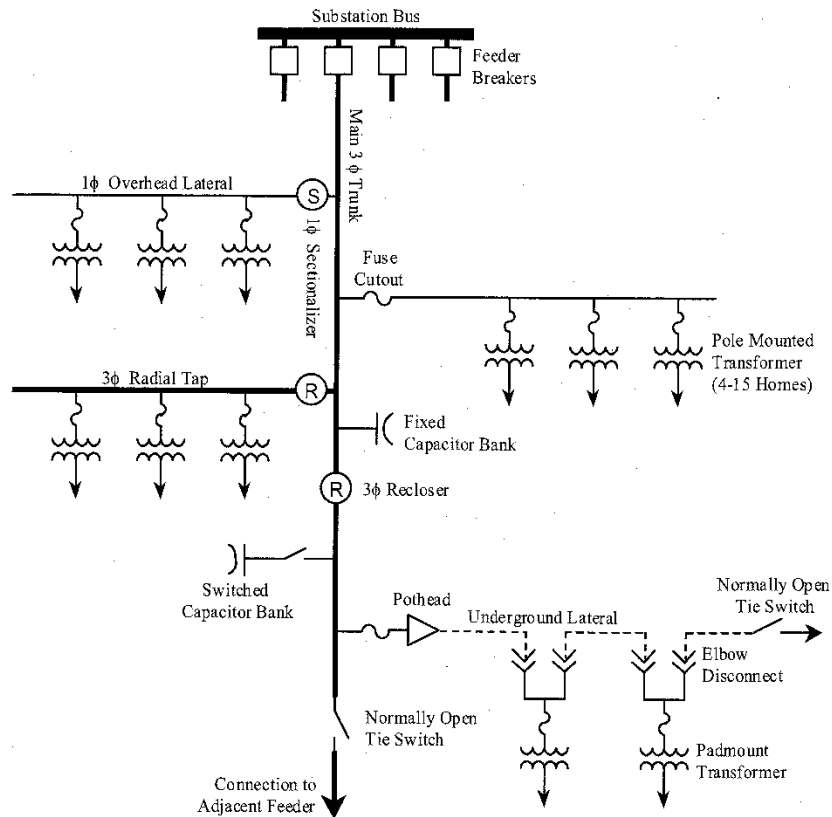


Figure 1.3 Typical Distribution System

1.2 Thesis Goals and Approach

Power system planners face a bevy of choices for system improvement and a limited amount of dollars. Does it make sense to spend millions of dollars building a new transmission line with large lattice steel towers or should those budget dollars be spent on

replacing aging power transformers? Should new “smart grid” technologies such as automated switches or automated metering take a higher priority? If a particular underground power cable configuration has been a problem, how much cable should be replaced and which locations are the most effective for improving reliability?

Questions such as these arise frequently and are only exacerbated by the fact that, in many utility organizational structures, the work groups requesting budget dollars for these projects have little or no overlap. These work groups exist as tiny islands trying to maximize the portion of the total budget allocated to them. The projects that these work groups request can vary widely and are very difficult to compare and prioritize. It is ultimately the responsibility of system planners, budget personnel, and executives to assemble and approve projects in the form of a capital budget. The main goal of this thesis is to provide a framework to assist these planners in efficiently allocating scarce budget dollars to maximize the reliability benefit.

It should be noted that there are obviously projects that will be done regardless of the reliability impact. Substations have to be built in order to meet projected load growth. Transmission lines and distribution circuits will emanate from these substations. Customers will request additional service or the relocation of existing services. These types of projects certainly exist but will not be further addressed in this work.

This project was in part inspired by the Federal Emergency Management Agency (FEMA) Pre-Disaster Mitigation (PDM) grant program. The basic idea behind this program is that FEMA found it was more cost-effective to address vulnerabilities through various mitigation activities prior to a disaster than it did to recover from that particular disaster. In the program, individual states compete for varying yearly amounts of grant dollars appropriated by Congress. States submit wide-ranging projects for consideration, such as flood mitigation, seismic retrofits, wildfire mitigation, tornado safe rooms, etc. All of these projects are evaluated on their technical merit and then compared with each other based upon their individual Benefit-Cost Ratio (BCR), simply the project benefits divided by the associated costs. Projects with high BCRs receive grant dollars; competing projects with lower BCRs are not funded. What is most interesting is that all of these projects from such different categories are evaluated on a common basis, the

BCR. This thesis applies these ideas to competing power system projects where the benefits are defined by the reliability improvements at the expense of constrained budget dollars.

1.3 Thesis Outline

This thesis will begin with a discussion on how power system reliability is defined; there are, perhaps surprisingly to the layperson, quite a few different ways a utility can measure reliability. Various indices and costs will be explained with a subsequent discussion of the pros and cons of each choice. The conversation will then segue into the background and concepts behind calculating the reliability of the respective portions of the power system – specifically the transmission, substation, and distribution systems. The transmission and substation system will be tied together with the distribution system through decoupled composite modeling. The background discussion will conclude with the method of comparing potential projects through the use of reliability benefit-cost analysis.

These concepts will then be applied to a hybrid system consisting of an actual transmission and substation system feeding a modified test system. The transmission system and substation come from a utility in the Southeastern United States that was energized in 1974. The distribution system comes from a widely used educational test system (Allan et al., 1991), modified appropriately to assist in the discussion. Circuit breaker operational failures will be modeled by interrupting medium through the use of Mean Cumulative Functions (MCFs); Poisson process models will be fitted appropriately. Other component modeling will be from appropriate industry sources.

The concepts will be applied to the hybrid system using the component information for a base case and the reliability results will then be calculated. This will then be followed by five different case studies including automating switches, replacing feeder breakers, replacing 3-Ø underground feeder cable, replacing 1-Ø Underground Residential Distribution (URD) cable, and finally 161 kV transmission system improvements to alleviate common-cause failure modes. The intent behind the choice of

these particular case studies is to provide at least one project option from the transmission, substation, and distribution systems.

The reliability of each case study will then be compared with the base case. The change in reliability in concert with the project cost for each project option will enable the reliability benefit-cost evaluations. All of the projects can then be ranked according to decreasing benefit-cost ratios. The projects are then grouped cumulatively, without interaction, by decreasing benefit cost to allow the utility to optimally choose a set of projects based upon a constrained capital budget allocation.

CHAPTER 2

LITERATURE REVIEW OF POWER SYSTEM RELIABILITY EVALUATION

2.1 Reliability and Reliability Cost Evaluation

What is the reliability benefit of a project? Is it reducing the frequency that customers experience outages? The duration of the outages? How about reducing the number of customers that experience an outage of a certain duration every year? Are all customers the same? That is to say, should a residential customer be treated the same as a large industrial customer that employs thousands of people? Reliability, as formally defined, is a number – specifically, it is the probability that a unit/device/system will be operating at some specified time (or cycles, miles, etc.) under stated design conditions. In this section, the various ways these ideas apply to power systems will be quantified formally and discussed in turn.

2.1.1 Power Industry Standards

The power industry uses a veritable alphabet soup of acronyms to measure the reliability of its systems. This section will focus only on the ones used most commonly. Customer interruptions can be classified as either momentary or sustained. IEEE 1366 places a threshold value of five minutes for the maximum momentary interruption before it is classified as a sustained outage. A momentary interruption could be caused by strong wind blowing a tree limb into a line, a recloser opening, the limb blowing clear, and the recloser holding at reset. Sustained outages are caused by short circuits and are the focus of this work. It should be noted, however, that there is an entire set of reliability indices devoted to the measurement of momentary interruptions, but they will

not be addressed further. The following are the most commonly used reliability indices with respective definitions taken from IEEE 1366:

System Average Interruption Frequency Index (SAIFI):

$$SAIFI = \frac{\text{Total \# of Customer Interruptions}}{\text{Total \# of Customers}} = \frac{\sum \lambda_i N_i}{\sum N_i} \quad \left(\frac{\text{int}}{\text{yr}}\right)$$

System Average Interruption Duration Index (SAIDI):

$$SAIDI = \frac{\sum \text{Customer Interruption Durations}}{\text{Total \# of Customers}} = \frac{\sum U_i N_i}{\sum N_i} \quad \left(\frac{\text{hr}}{\text{yr}}\right)$$

Customer Average Interruption Duration Index (CAIDI):

$$CAIDI = \frac{\sum \text{Customer Interruption Durations}}{\text{Total \# of Customer Interruptions}} = \frac{\sum U_i N_i}{\sum \lambda_i N_i} \quad (\text{hr})$$

where:

λ_i = expected annual failure rate and load point i

N_i = number of customers at load point i

U_i = expected annual outage duration at load point i

SAIFI measures the average number of sustained interruptions an average customer would see per year. SAIDI measures the total expected duration of sustained interruption hours an average customer would experience per year. CAIDI measures how long it takes, on average, to address a given sustained interruption by the utility.

Several things should be pointed out. SAIFI, SAIDI, and CAIDI treat all customers – residential, commercial, and industrial – equally. A single home experiencing an outage that spoils food in the refrigerator is equivalent to a large industrial customer that could lose hundreds of thousands of dollars in that same outage from a bad manufacturing cycle. For a constant (or functionally constant given low growth rate changes) customer base, the only way to improve SAIFI is to reduce the number of interruptions. SAIDI can be improved by either reducing the number of interruptions or by improving the duration or response to an interruption. It also should be noted that SAIFI & SAIDI, while typically used globally at the system level, can also be used locally at the substation, feeder, tap level, etc.

This thesis will also use an alternate reliability measure, CMI, which is Customer-Minutes Interrupted. It is simply the numerator of SAIDI without normalizing for a certain customer set. Its use is convenient for comparing projects that affect different numbers of customers.

2.1.2 Minimization of Societal Costs

Societal costs of reliability consist of the sum of customer and utility costs. Brown (2009) presents a set of generic customer, utility, and total cost curves versus reliability as shown in Figure 2.1. The minimum point on the total cost curve represents the point of optimal social welfare by minimizing total societal costs.

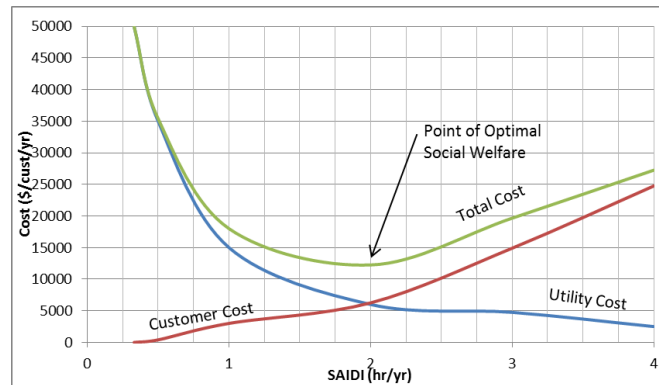


Figure 2.1 Total Societal Costs

The societal costs associated with an outage consist of the sum of the outage cost to the customer and to the utility. Consider a breaker operational failure scenario, using Figure 1.2 as a reference, in which one of the feeder breaker trips open and then fails to close. Operations will determine that the breaker has in fact failed open. A troubleshooter will be dispatched to transfer load by manually operating appropriate switches (i.e., by manually opening a switch just outside station on the load side of the breaker and then by manually closing a tie switch on an adjacent feeder with sufficient transfer capacity). All of the customers on that feeder will experience an outage during

this manual switching routine; customers not able to be restored by switching will experience an outage minimally equal to the duration of breaker repair. Customers will experience a cost associated with the outage and the utility will lose revenue during the outage. Breaker maintenance crews will be called out to repair the breaker. After the breaker is repaired, the system is then returned back to its initial state by another round of switching. The total cost of an outage due to failure can therefore be summarized as follows:

$$C_{Failure} = C_{Customer\ Outage} + C_{Utility\ Repair} + C_{Utility\ Switching} + C_{Lost\ Utility\ Revenue}$$

The customer costs associated with an outage obviously depend on many factors. The cost of a one-hour outage to a residential customer is obviously much lower than to a large commercial or industrial customer employing hundreds or thousands of employees with annual demands of thousands of kW. Outage costs also depend on outage duration, season, time of day, etc. These costs have been quantified in Customer Damage Functions (CDFs) by Lawton et al. (2003). This study, which built on the Electric Power Research Institute (EPRI) “Outage Cost Estimation Guidebook” (1995), used 24 datasets recorded from 12 major electric utilities across the United States during the period from 1989-2002. The datasets used customer cost surveys to estimate outage costs. Residential customers were asked how much they were Willing to Pay (WTP) to avoid outages of differing characteristics (duration, season, time of year, etc.); commercial and industrial customers were also asked to estimate their direct costs associated with outages of differing characteristics. Ultimately, CDFs were modeled based upon three distinct customer types – residential, small Commercial and Industrial (C&I; those with <1 MW peak demand), and large C&I (>1 MW peak demand). These CDFs are now presented here for a generic utility in the Southeastern United States. A supplemental file to this thesis (File 1, cdf_coefficients.xls) displays the associated regression coefficients.

Residential Customer Damage Function:

$$\ln(y) = c_0 + c_1x_1 + c_2x_1^2 + c_3x_2 + c_4x_3 + c_5x_5 + c_6x_5 + c_7x_6 + c_8x_7 + c_9x_8$$

where:

y = Outage cost for a generic residential customer

c_i = fitted regression coefficient (File 1, cdf_coefficients.xls)

x_1 = outage duration (hours)

x_2 = morning indicator variable (0 or 1)

x_3 = night indicator variable (0 or 1)

x_4 = weekend indicator variable (0 or 1)

x_5 = winter indicator variable (0 or 1)

x_6 = Southeast indicator variable (0 or 1)

x_7 = annual MWh

x_8 = $\ln(\text{annual household income, \$})$

This model therefore predicts that a generic residential customer in the Southeast U.S. (average annual usage of 14,300 kWh; annual income \$40,180) is willing to pay ~\$4.38 to avoid a 1-hour duration outage on a summer weekday afternoon.

The CDF for commercial & industrial customers represents direct costs associated with an outage. The CDF for small Commercial & Industrial customers (<1 MW annual peak demand) is presented here:

Small Commercial & Industrial (<1 MW peak demand) Customer Damage Function:

$$\ln(y) = c_0 + c_1x_1 + c_2x_1^2 + c_3x_2 + c_4x_3 + c_5x_1x_3 + c_6x_4 + c_7x_5 + c_8x_6 + c_9x_7$$

where:

y = Outage cost for a generic small C&I customer

c_i = fitted regression coefficient (File 1, cdf_coefficients.xls)

x_1 = outage duration (hours)

x_2 = number of employees

x_3 = annual kWh

x_4 = morning indicator variable (0 or 1)

x_5 = night indicator variable (0 or 1)

x_6 = weekend indicator variable (0 or 1)

x_7 = winter indicator variable (0 or 1)

This model therefore predicts that a generic small commercial or industrial customer (<1 MW peak demand) experiences direct costs of ~\$1,200 for a 1-hour duration outage on a summer weekday afternoon. The average small C&I customer from the study had an annual kWh usage of ~12,000 kWh and ~120 employees. Generally, most C&I customers do not employ 120 people; however, the model isn't as sensitive to changes in the number of employees as to other factors. For example, changing the number of employees from 120 to 20 while holding all other factors constant reduces the 1-hr outage cost listed above from ~\$1,200 to ~\$1,000.

The CDF for large Commercial & Industrial customers (>1 MW peak demand) is presented here:

Large Commercial & Industrial Customer Damage Function

$$\ln(y) = c_0 + c_1x_1 + c_2x_1^2 + c_3x_2 + c_4x_3 + c_5x_1x_3 + c_6x_4 + c_7x_5 + c_8x_6 + c_9x_7$$

where:

y = Outage cost for a generic large C&I customer

c_i = fitted regression coefficient (File 1, cdf_coefficients.xls)

x_1 = outage duration (hours)

x_2 = number of employees

x_3 = annual kWh

x_4 = morning indicator variable (0 or 1)

x_5 = night indicator variable (0 or 1)

x_6 = weekend indicator variable (0 or 1)

x_7 = winter indicator variable (0 or 1)

This model therefore predicts that a generic large commercial or industrial customer experiences direct costs of ~\$8,200 for a 1-hour duration outage on a summer weekday afternoon. The average large C&I customer from the study had an annual usage of 17.5 million kWh and had 373 employees.

It should be noted that these CDFs are for generic customer types only and do not reflect the actual, specific costs to an individual customer.

2.1.3 Benefits & Drawbacks of Each Method

Choosing between using a standard power industry reliability index or societal cost minimization for project prioritization ultimately reflects a utility philosophical choice. There are issues with each method. Brown (2009) collects and presents the main arguments against minimizing societal costs. First is the obvious problem that cost surveys present. It is highly unlikely that a residential customer would actually be willing to pay ~\$5 to avoid an outage; similarly, C&I customers will overstate their outage costs, particularly if those customers are aware that reliability improvement projects will be based upon the survey results. Second, a business physically located in an area where reliability improvements are not cost effective by this method could effectively subsidize the profits of a competitor located in an area where reliability improvements are cost effective as both customers pay the same rate. Finally, customers who can make more cost effective reliability improvements to their own facilities (emergency generators, uninterruptible power supplies, etc.) obviously prefer that the utility make improvements on the utility side to address the problem, often at much higher cost. Conversely, it seems unreasonable to equate a residential and C&I customer outage experience. Ultimately, Brown argues against minimizing societal cost and encourages setting reasonable reliability standards and making customers pay for reliability improvements above these minimum standards. This thesis will present the results from both methods but ultimately will use \$/CMI as the basis for comparison.

2.2 System Reliability Evaluation

A primer on the methods used in reliability analysis is now presented. The forthcoming sections rely heavily and use conceptual examples from Billinton (1992), Billinton (2012) and Billinton et al. (1978). First, an introduction to discrete Markov chains using a simple two-state system is presented. Building on this section, an overview of continuous-time Markov processes with multiple components and multiple states follows. A discussion of series-parallel arrangements will then follow.

2.2.1 Discrete Markov Chains

The basic idea behind Markov techniques is that components or systems reside in and transition between states. These transitions can occur in discrete steps or vary continuously; however the transition rate between states is constant (i.e., a stationary process). Also key to Markov techniques is that the future state of the component depends only on the current state (i.e., memoryless). Consider the simple two-state system shown in Figure 2.2. The two states – State 1 and State 2 – could be “up” or “down” or some other appropriate description.

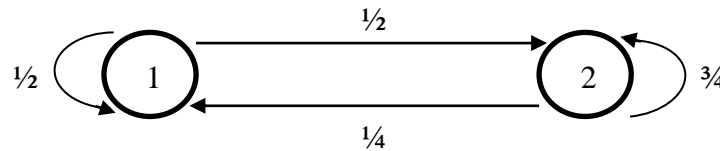


Figure 2.2 Two State System

Assume initially that the system shown in Figure 2.2 is in State 1 (up). It will transition to State 2 (down) with probability of $\frac{1}{2}$, or it will remain in State 1 with probability of $\frac{1}{2}$. What is important is that the sum of the probabilities is unity (i.e., the system either remains in its current state or transitions to some other state). Similarly, the system will remain in State 2 with probability of $\frac{3}{4}$ or transition to State 1 with

probability of $\frac{1}{4}$. If we were to transition forward multiple steps, we could diagram the potential outcomes of the system. This is shown in the tree diagram of Figure 2.3.

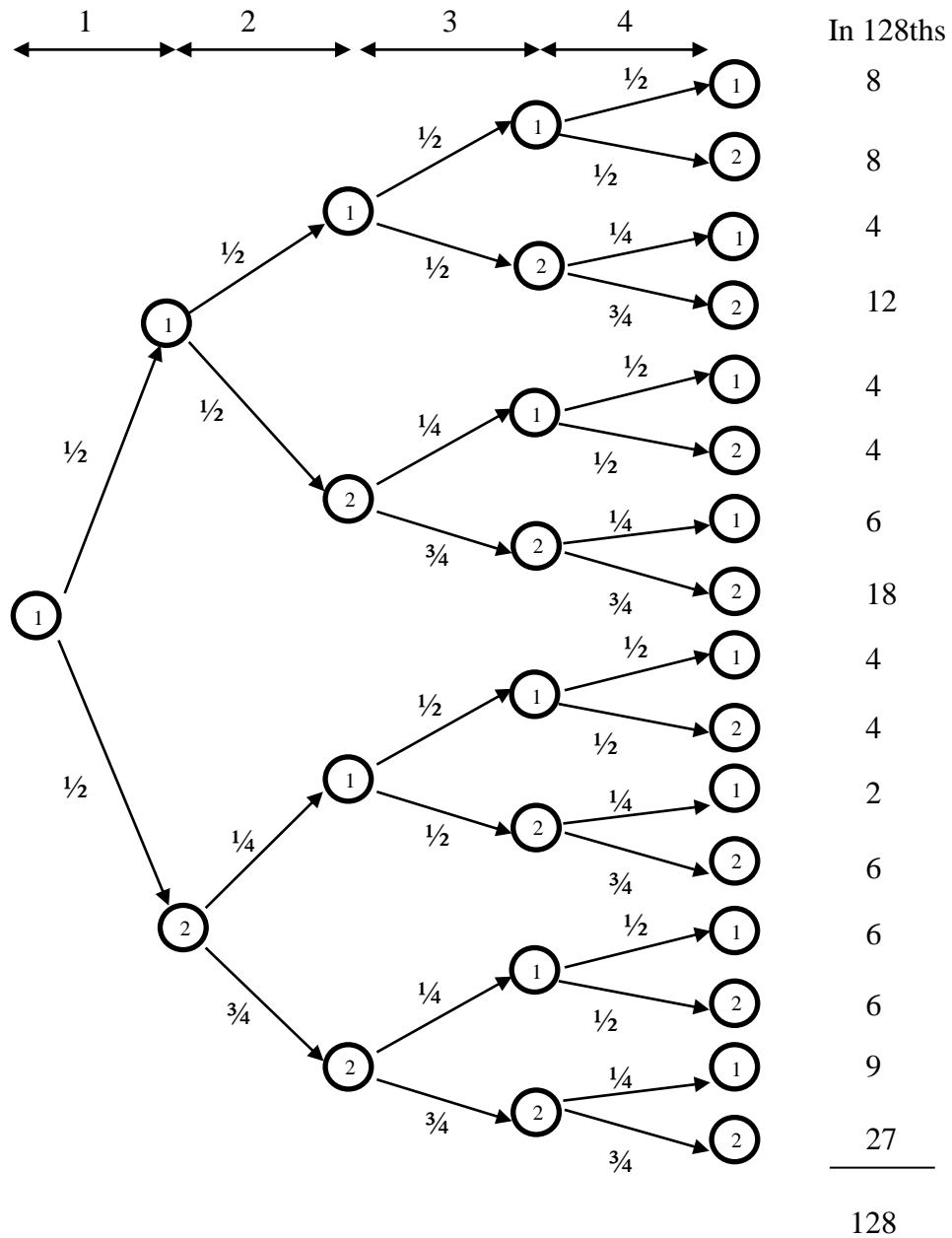


Figure 2.3 Tree Diagram

The system is assumed to initially be in State 1; the tree diagram represents four time steps into the future with resulting path probabilities (given in 128ths). Again, the total probability of being in any state is 1(128/128) as required.

Table 2.1 below sums the probabilities of being in either State 1 or State 2 for each time interval. These are then plotted in Figure 2.4 with blue being State 1.

Table 2.1 State Probabilities

Time Interval	State 1	State 2
1	$1/2 = 0.5$	$1/2 = 0.5$
2	$3/8 = 0.375$	$5/8 = 0.625$
3	$11/32 = 0.344$	$21/32 = 0.656$
4	$43/128 = 0.336$	$85/128 = 0.664$
5	$171/512 = 0.334$	$341/512 = 0.666$

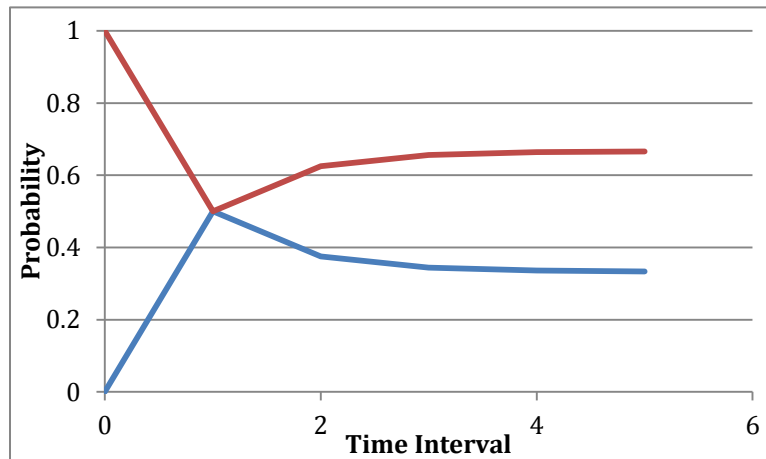


Figure 2.4 Steady-State Probabilities

What is key here is that the system reaches a steady-state probability of being in a certain state. It is also important to note that the system reaches these steady-state conditions regardless of the starting condition (“up” or “down”). This behavior is consistent with ergodic systems.

The simple two state system in Figure 2.2 can be represented in matrix notation as shown by the following matrix **P**:

$$\mathbf{P} = \begin{bmatrix} P_{11} & P_{12} \\ P_{21} & P_{22} \end{bmatrix} = \begin{bmatrix} 1/2 & 1/2 \\ 1/4 & 3/4 \end{bmatrix}$$

where P_{ij} = probability of making a transition to state j after a time interval given that it was in state i at the beginning of the time interval.

Matrix **P** shows that the probability of staying in State 1 given that it is currently in State 1 is $1/2$; the probability of moving to State 1 given that it is currently in State 2 is $1/4$ and so forth. This is known as a stochastic transitional probability matrix. The rows of the matrix can be read as the “from” state and moving along the columns to the right can be read as “to” state.

If we were to move one time interval into the future, we would simply multiply the matrix **P** by itself as follows:

$$\mathbf{P}^2 = \begin{bmatrix} P_{11} & P_{12} \\ P_{21} & P_{22} \end{bmatrix} \begin{bmatrix} P_{11} & P_{12} \\ P_{21} & P_{22} \end{bmatrix} = \begin{bmatrix} 1/2 & 1/2 \\ 1/4 & 3/4 \end{bmatrix} \begin{bmatrix} 1/2 & 1/2 \\ 1/4 & 3/4 \end{bmatrix} = \begin{bmatrix} 3/8 & 5/8 \\ 5/16 & 11/16 \end{bmatrix}$$

This can be interpreted as the probability of being in State 1 after one time interval given that it started in State 1 is $3/8$; the probability of being in State 2 after one time interval given that it started in State 1 is $5/8$. These results match those in Table 2.1 and Figure 2.4. The second row of the above matrix gives the results that would be found if we were to assume that the initial condition was State 2. If the initial starting condition is assumed to start in State 1 represented by a vector then the above can similarly be rewritten as:

$$\mathbf{P}(0) = [1 \quad 0]$$

and the above narrative can similarly be rewritten as:

$$\mathbf{P}(2) = \mathbf{P}(0)\mathbf{P}^2 = \begin{bmatrix} 1 & 0 \end{bmatrix} \begin{bmatrix} 3/8 & 5/8 \\ 5/16 & 11/16 \end{bmatrix} = \begin{bmatrix} 3/8 & 5/8 \end{bmatrix}$$

This then leads to the description of the system n-steps into the future as:

$$\mathbf{P}(n) = \mathbf{P}(0)\mathbf{P}^n$$

Consider again that what we are interested in is the steady-state behavior of the system.

Ergodic systems can be written as follows:

$$\boldsymbol{\pi}\mathbf{P} = \boldsymbol{\pi}$$

where $\boldsymbol{\pi}$ represents the steady-state probability vector and \mathbf{P} represents the stochastic transition probability matrix. The idea behind the above equation is that over time, no matter how many time intervals projected into the future the same result will be obtained. This can then be reduced as follows:

$$\mathbf{P}^T \boldsymbol{\pi}^T = \boldsymbol{\pi}^T$$

$$\begin{bmatrix} 1/2 & 1/4 \\ 1/2 & 3/4 \end{bmatrix} \begin{bmatrix} \pi_1 \\ \pi_2 \end{bmatrix} = \begin{bmatrix} \pi_1 \\ \pi_2 \end{bmatrix}$$

resulting in the following equations:

$$\begin{aligned} 1/2\pi_1 + 1/4\pi_2 &= \pi_1 \\ 1/2\pi_1 + 3/4\pi_2 &= \pi_2 \end{aligned}$$

which then reduce to following:

$$1/2\pi_1 = 1/4\pi_2$$

$$1/2\pi_1 = 1/4\pi_2$$

These are equivalent resulting in one equation and two unknowns. Remember that the sum of the probabilities must be unity, so our second equation is:

$$\pi_1 + \pi_2 = 1$$

This then results in the following steady-state probabilities:

$$\pi_1 = 1/3$$

$$\pi_2 = 2/3$$

This result is consistent with those given in Table 2.1 and Figure 2.4.

2.2.2 Continuous Markov Processes

The same ideas in the previous section can now be applied to systems where the transitions (i.e., failures and repairs) can be associated with a probability distribution. As the transition rates for Markov processes must be constant, this implies that these failure and repair times are distributed exponentially. Consider again the single repairable component two-state system as before but now with failure rate λ and repair rate μ as shown in Figure 2.5:

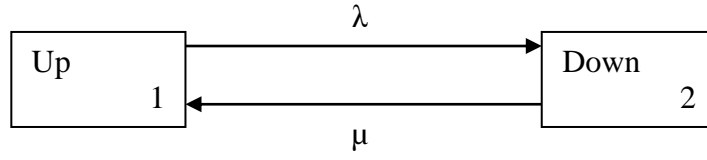


Figure 2.5 Two-State Continuous Model

Recall that the density function for the exponential distribution is $f(t)=\lambda e^{-\lambda t}$. So the density functions for the up and down times for this single repairable component system are:

$$f_1(t) = \lambda e^{-\lambda t}$$

$$f_2(t) = \mu e^{-\mu t}$$

where $\lambda = 1/\text{MTTF}$ (Mean Time To Failure) and $\mu = 1/\text{MTTR}$ (Mean Time To Repair). The time-dependent probabilities of being found in the up or down state are given by Billinton (1992) as:

$$P_1(t) = \frac{\mu}{\lambda + \mu} + \frac{\lambda e^{-(\lambda + \mu)t}}{\lambda + \mu}$$

$$P_2(t) = \frac{\lambda}{\lambda + \mu} + \frac{\lambda e^{-(\lambda + \mu)t}}{\lambda + \mu}$$

The steady-state probabilities (i.e., as $t \rightarrow \infty$) for this single repairable component system are therefore:

$$P_1 = \frac{\mu}{\lambda + \mu}$$

$$P_2 = \frac{\lambda}{\lambda + \mu}$$

It should be noted that the stochastic transitional probability matrix for the system in Figure 2.5 can be setup as before with the introduction of a small time interval Δt , where the probability of failure in the interval Δt is $\lambda\Delta t$ and the probability of no failure in the interval is $1-\lambda\Delta t$. It should be noted that the interval Δt is so small that the probability of two or more transitions in the interval is negligible. Billinton (1992) shows that the Δt term drops out, ultimately reducing to the equations above.

We can now extend these ideas to two repairable component system, with each component having two states. It is assumed that the component failures are independent – i.e., a failure of one component has no effect on the other component. This system would therefore have four total states as shown in Figure 2.6:

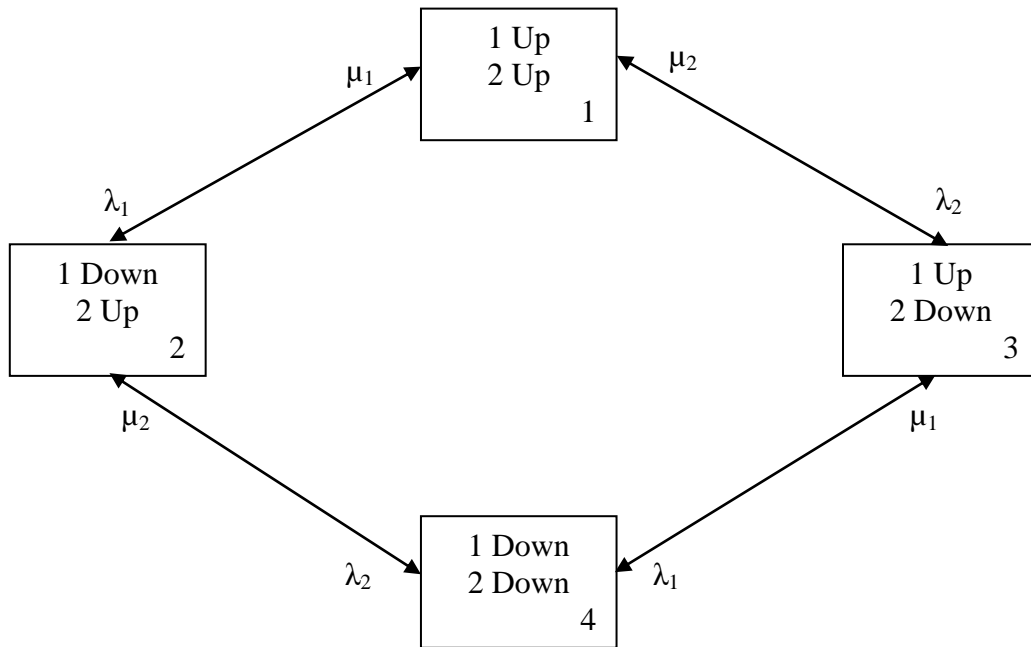


Figure 2.6 Two Component Repairable System

For a series system, the up (Availability) state would be State 1 and the down (Unavailability) states would States 2, 3 & 4 (i.e., the probability of being down is the

sum of the probabilities of States 2, 3 & 4). For parallel systems, as in the case of the multiple transmission feeds that we are interested in, the down state is State 4 and the up states are States 1, 2 & 3.

The parallel transmission feeds for each substation can now be modeled as above, where the “component” is a transmission circuit with respective failure rate and repair rate. In this instance we would only be interested in State 4 as both circuits would be down and the station would be completely outaged.

The resulting stochastic transitional probability matrix \mathbf{P} is therefore:

$$\mathbf{P} = \begin{bmatrix} 1 - \lambda_1 - \lambda_2 & \lambda_1 & \lambda_2 & 0 \\ \mu_1 & 1 - \lambda_2 - \mu_1 & 0 & \lambda_2 \\ \mu_2 & 0 & 1 - \lambda_1 - \mu_2 & \lambda_1 \\ 0 & \mu_2 & \mu_1 & 1 - \mu_1 - \mu_2 \end{bmatrix}$$

As before, we are interesting in finding the steady-state probability vector $\boldsymbol{\pi}$:

$$\mathbf{P}^T \boldsymbol{\pi}^T = \boldsymbol{\pi}^T$$

$$\begin{bmatrix} 1 - \lambda_1 - \lambda_2 & \mu_1 & \mu_2 & 0 \\ \lambda_1 & 1 - \lambda_2 - \mu_1 & 0 & \mu_2 \\ \lambda_2 & 0 & 1 - \lambda_1 - \mu_2 & \mu_1 \\ 0 & \lambda_2 & \lambda_1 & 1 - \mu_1 - \mu_2 \end{bmatrix} \begin{bmatrix} \pi_1 \\ \pi_2 \\ \pi_3 \\ \pi_4 \end{bmatrix} = \begin{bmatrix} \pi_1 \\ \pi_2 \\ \pi_3 \\ \pi_4 \end{bmatrix}$$

Billinton & Allan (1992) provide the steady-state probabilities as follows:

$$\pi_1 = \frac{\mu_1 \mu_2}{(\lambda_1 + \mu_1)(\lambda_2 + \mu_2)}$$

$$\pi_2 = \frac{\lambda_1 \mu_2}{(\lambda_1 + \mu_1)(\lambda_2 + \mu_2)}$$

$$\pi_3 = \frac{\mu_1 \lambda_2}{(\lambda_1 + \mu_1)(\lambda_2 + \mu_2)}$$

$$\pi_4 = \frac{\lambda_1 \lambda_2}{(\lambda_1 + \mu_1)(\lambda_2 + \mu_2)}$$

For systems with multiple components, the resulting number of states makes the use of Markov techniques unwieldy. For example, a system with five components, each with only an “up” and a “down” state, will result in $2^5 = 32$ different system states. As such, approximations using these techniques as a base are necessary.

2.2.3 Series Systems

Recall from Section 2.2.2 that the single component up (available) state probability was given as:

$$P_{up} = \frac{\mu}{\lambda + \mu}$$

For a two-component system, the up state was State 1 with probability:

$$\pi_1 = \frac{\mu_1 \mu_2}{(\lambda_1 + \mu_1)(\lambda_2 + \mu_2)}$$

Consider the system given in Figure 2.7 showing a two-component series system and an equivalent single component system:



Figure 2.7 Equivalent Series System

For the two systems to be equivalent:

$$\frac{\mu_1 \mu_2}{(\lambda_1 + \mu_1)(\lambda_2 + \mu_2)} = \frac{\mu_s}{\lambda_s + \mu_s}$$

And the equivalent transition rate $\lambda_s = \lambda_1 + \lambda_2$. Using an equivalent average repair time, r_s , as the reciprocal of the repair rate, μ_s , results in the following:

$$r_s = \frac{1}{\mu_s} = \frac{\lambda_1 r_1 + \lambda_2 r_2 + \lambda_1 \lambda_2 r_1 r_2}{\lambda_s}$$

where the $\lambda_1 \lambda_2 r_1 r_2$ term is usually much, much smaller than either $\lambda_1 r_1$ or $\lambda_2 r_2$ and is therefore usually ignored, resulting in the following:

$$r_s = \frac{\lambda_1 r_1 + \lambda_2 r_2}{\lambda_s}$$

For an n-component series system, the failure rate can be expressed as:

$$\lambda_s = \sum_{i=1}^n \lambda_i$$

which is usually expressed in failures/year. This can be interpreted to mean that the failure of the system results from the failure of any component. The system unavailability, U_s , is equal to the sum of products of the down state frequency and repair times, i.e.:

$$U_s = \sum_{i=1}^n \lambda_i r_i$$

where U_s is usually expressed as hours per year (h/yr). The average repair time can therefore be calculated as:

$$r_s = \frac{U_s}{\lambda_s}$$

where r_s is usually expressed in hours.

2.2.4 Parallel Systems

Recall from Section 2.2.2 that the single component down (Unavailable) state probability was given as:

$$P_{down} = \frac{\lambda}{\lambda + \mu}$$

For a two-component system, the down state was State 4 with probability:

$$\pi_4 = \frac{\lambda_1 \lambda_2}{(\lambda_1 + \mu_1)(\lambda_2 + \mu_2)}$$

Consider the system given in Figure 2.8 showing a two-component parallel system and an equivalent single component system:

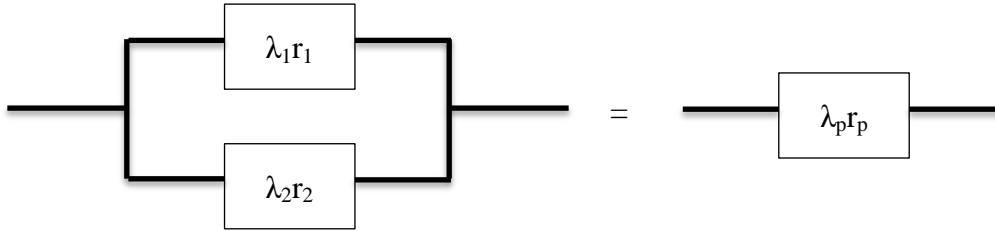


Figure 2.8 Equivalent Parallel System

For the two systems to be equivalent:

$$\frac{\lambda_1 \lambda_2}{(\lambda_1 + \mu_1)(\lambda_2 + \mu_2)} = \frac{\lambda_p}{\lambda_p + \mu_p}$$

and the equivalent transition rate from the down state is $\mu_p = \mu_1 + \mu_2$. This can equivalently be stated using average repair times as:

$$\frac{1}{r_p} = \frac{1}{r_1} + \frac{1}{r_2}$$

$$r_p = \frac{r_1 r_2}{r_1 + r_2}$$

This then results in the following equivalent expression for a two-component parallel system:

$$\lambda_p = \frac{\lambda_1 \lambda_2 (r_1 + r_2)}{1 + \lambda_1 r_1 + \lambda_2 r_2}$$

and since $\lambda_1 r_1$ and $\lambda_2 r_2$ are usually $\ll 1$, this reduces to :

$$\lambda_p = \lambda_1 \lambda_2 (r_1 + r_2) = \lambda_1 (\lambda_2 r_1) + \lambda_2 (\lambda_1 r_2)$$

This can be interpreted to mean that the system will fail if component 2 fails while component 1 is being repaired subsequent to failure or component 1 fails while component 2 is being repaired subsequent to failure. The system unavailability, U_p , is equal to the sum of products of the down state frequency and repair times, i.e.:

$$U_p = \lambda_p r_p = \lambda_1 \lambda_2 r_1 r_2$$

This logic can be extended to systems with more than two components in parallel.

2.2.5 Combined Series-Parallel Systems

Many systems have configurations involving components in both series and parallel or even more complex bridge networks. Network reduction is commonly used for series-parallel systems. This method involves combining or reducing the combinations of the system that are in series or parallel until the system can be expressed

as a single equivalent component. This process and the resulting equations can become quite involved and tedious for larger, complex systems. Another drawback to this method is that it is sometimes not obvious which component (or set of components) contributes the most to overall system unreliability.

A method that does make clear the magnitude of the unreliability contribution of each component or set of components is Failure Mode and Effects Analysis (FMEA). The failure modes of the components contribute to minimum cut sets, which are defined as the “set of system components which, when failed, cause failure of the system” (Billinton & Allan, 1992). In many power systems, these minimum cut sets can be evaluated by inspection, although algorithms do exist for their development from more complex systems. Because each minimum cut set guarantees system failure, each of the cut sets can be thought of as equivalent blocks in series. Each respective cut set is evaluated for its failure rate, repair time, and unavailability using the series/parallel methods as described in previous sections depending on the components in the cut set. As the cut sets are in series, the overall system failure rate and unavailability is calculated as for a series system.

It should be noted that this method provides an upper bound to system unreliability. The reason is that the FMEA approach uses the approximation as discussed in previous sections; the lower bound can be found by subtracting the product of the event unreliability pairs. This is generally unnecessary as the difference is negligible if $\lambda r \ll 1$ for each component, as is usually the case in power system evaluation.

As a simple example of the ideas expressed in this section, consider the series-parallel system in Figure 2.9:

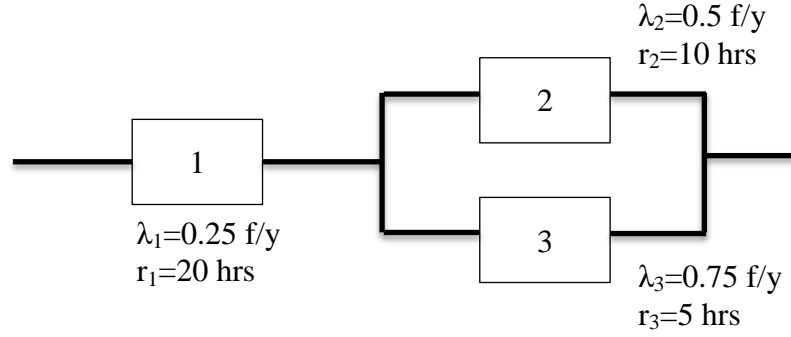


Figure 2.9 Combined Series-Parallel System

Using network reduction, components 2 & 3 are first reduced into an equivalent component as follows:

$$\lambda_{23} = \lambda_2 \lambda_3 (r_2 + r_3) = (0.5 \text{ f / yr})(0.75 \text{ f / yr}) \left[\frac{(10 \text{ hrs} + 5 \text{ hrs})}{8760 \text{ hrs / yr}} \right] = 6.42 \times 10^{-4} \text{ f / yr}$$

$$r_{23} = \frac{r_2 r_3}{r_2 + r_3} = \frac{(10 \text{ hrs})(5 \text{ hrs})}{(10 \text{ hrs} + 5 \text{ hrs})} = 3.33 \text{ hrs}$$

$$U_{23} = \lambda_{23} r_{23} = (6.42 \times 10^{-4} \text{ f / yr})(3.33 \text{ hrs}) = 0.00214 \text{ hrs / yr}$$

This equivalent component is then combined with the Series component 1 as follows:

$$\lambda_{\text{sys}} = \lambda_1 + \lambda_{23} = 0.25 \text{ f / yr} + 6.42 \times 10^{-4} \text{ f / yr} = 0.250642 \text{ f / yr}$$

$$U_{\text{sys}} = \lambda_1 r_1 + \lambda_{23} r_{23} = (0.25 \text{ f / yr})(20 \text{ hrs}) + (6.42 \times 10^{-4} \text{ f / yr})(3.33 \text{ hrs}) = 5.00214 \text{ hrs}$$

$$r_{\text{sys}} = \frac{U_{\text{sys}}}{\lambda_{\text{sys}}} = \frac{5.00214 \text{ hrs / yr}}{0.250642 \text{ f / yr}} = 19.96 \text{ hrs}$$

Similarly, the system can be evaluated using FMEA. The minimum cut sets of the system are {1} and {2,3}. The failure rate, repair time, and unavailability are calculated for each cut set with results shown in Table 2.2:

Table 2.2 System Reliability of Figure 2.9 using FMEA

Min Cut Set	λ (f/yr)	r (hrs)	U (hrs/yr)
1	0.25	20	5
2 and 3	6.42×10^{-4}	3.33	0.00214
Total	0.250642	19.96	5.00214

where $\lambda_{\text{total}} = \sum \lambda_i$; $U_{\text{total}} = \sum U_i$; $r_{\text{total}} = U_{\text{total}} / \lambda_{\text{total}}$

As can be seen from Table 2.2, the results from both methods are the same. FMEA, however, clearly shows that component 1 dominates the system unreliability, as would be expected as it is a series component.

2.3 Transmission System Assessment

Transmission lines will be evaluated in this thesis as repairable components in accordance with the Markov techniques described in Section 2.2.2, with one main difference. An additional failure event, which results in both lines being down known as a common-cause failure mode, will be added. It is not uncommon for a single transmission tower to carry multiple transmission circuits. The loss of a single tower due to vehicle impacts, flood, etc., will therefore result in the loss of both circuits. The IEEE Subcommittee on the Application of Probability Methods recognized the importance of this failure mode and commissioned a Task Force on its study (IEEE 1976). The Task Force defined a common-cause failure as “an event having a single external cause with multiple failure events where the events are not consequences of each other.”

The resulting model accounting for this common-cause failure mode is shown in Figure 2.10.

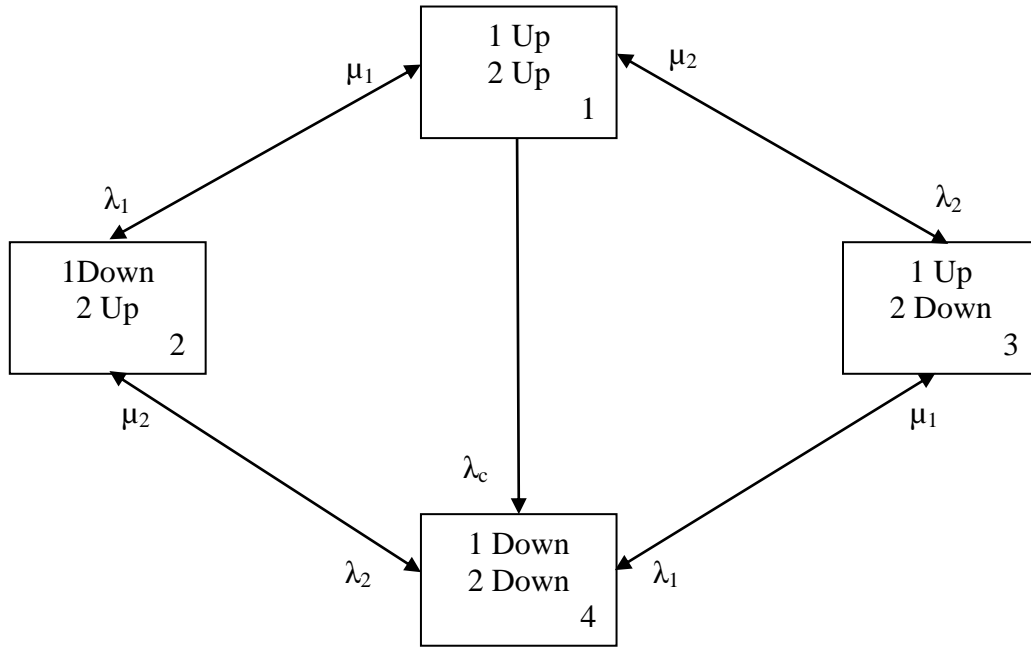


Figure 2.10 State Space Diagram w/Common Cause Failures

The common-cause failure mode is accounted for in Figure 2.10 by λ_c . This is the model that will be used in the forthcoming analysis. It is important to note, therefore, what this model says and what it does not say. It assumes that the transmission lines are not identical; each line has its own distinct failure and repair characteristics. It also assumes that there is a common-cause failure mode that will cause both lines to be outaged at once. This common-cause failure mode is distinct from a simultaneous failure, $\lambda_1\lambda_2$, of the two lines independently. It does not say, in the case that there is a common-cause failure, that both lines would be able to be repaired at exactly the same time (i.e., a common-cause repair). It assumes that each line would have to be repaired separately.

The resulting stochastic transitional probability matrix \mathbf{P} is therefore:

$$\mathbf{P} = \begin{bmatrix} 1 - \lambda_1 - \lambda_2 - \lambda_c & \lambda_1 & \lambda_2 & \lambda_c \\ \mu_1 & 1 - \lambda_2 - \mu_1 & 0 & \lambda_2 \\ \mu_2 & 0 & 1 - \lambda_1 - \mu_2 & \lambda_1 \\ 0 & \mu_2 & \mu_1 & 1 - \mu_1 - \mu_2 \end{bmatrix}$$

As before, we are interesting in finding the steady-state probability vector $\boldsymbol{\pi}$:

$$\mathbf{P}^T \boldsymbol{\pi}^T = \boldsymbol{\pi}^T$$

$$\begin{bmatrix} 1 - \lambda_1 - \lambda_2 - \lambda_c & \mu_1 & \mu_2 & 0 \\ \lambda_1 & 1 - \lambda_2 - \mu_1 & 0 & \mu_2 \\ \lambda_2 & 0 & 1 - \lambda_1 - \mu_2 & \mu_1 \\ \lambda_c & \lambda_2 & \lambda_1 & 1 - \mu_1 - \mu_2 \end{bmatrix} \begin{bmatrix} \pi_1 \\ \pi_2 \\ \pi_3 \\ \pi_4 \end{bmatrix} = \begin{bmatrix} \pi_1 \\ \pi_2 \\ \pi_3 \\ \pi_4 \end{bmatrix}$$

Billinton (1978) provides the steady-state probabilities as follows:

$$\pi_1 = \frac{\mu_1 \mu_2 (\lambda_1 + \lambda_2 + \mu_1 + \mu_2)}{(\lambda_1 + \mu_1)(\lambda_2 + \mu_2)(\lambda_1 + \lambda_2 + \mu_1 + \mu_2) + \lambda_c [(\lambda_1 + \mu_1)(\lambda_2 + \mu_1 + \mu_2) + \mu_2(\lambda_2 + \mu_2)]}$$

$$\pi_2 = \frac{\mu_2 [\lambda_1 (\lambda_1 + \lambda_2 + \mu_1 + \mu_2) + \lambda_c (\lambda_1 + \mu_2)]}{(\lambda_1 + \mu_1)(\lambda_2 + \mu_2)(\lambda_1 + \lambda_2 + \mu_1 + \mu_2) + \lambda_c [(\lambda_1 + \mu_1)(\lambda_2 + \mu_1 + \mu_2) + \mu_2(\lambda_2 + \mu_2)]}$$

$$\pi_3 = \frac{\mu_1 [\lambda_2 (\lambda_1 + \lambda_2 + \mu_1 + \mu_2) + \lambda_c (\lambda_2 + \mu_1)]}{(\lambda_1 + \mu_1)(\lambda_2 + \mu_2)(\lambda_1 + \lambda_2 + \mu_1 + \mu_2) + \lambda_c [(\lambda_1 + \mu_1)(\lambda_2 + \mu_1 + \mu_2) + \mu_2(\lambda_2 + \mu_2)]}$$

$$\pi_4 = \frac{\lambda_1 \lambda_2 (\lambda_1 + \lambda_2 + \mu_1 + \mu_2) + \lambda_c (\lambda_1 + \mu_2)(\lambda_2 + \mu_1)}{(\lambda_1 + \mu_1)(\lambda_2 + \mu_2)(\lambda_1 + \lambda_2 + \mu_1 + \mu_2) + \lambda_c [(\lambda_1 + \mu_1)(\lambda_2 + \mu_1 + \mu_2) + \mu_2(\lambda_2 + \mu_2)]}$$

2.4 Substation System Assessment

The concepts introduced in the previous sections will now be extended to the substation system. Certain components, particularly circuit breakers, in the substation have different modes of failure which have to be taken into account in the FMEA analysis. Consider again the substation shown in Figure 1.2, which is reproduced here in Figure 2.11 as a simplified one-line diagram:

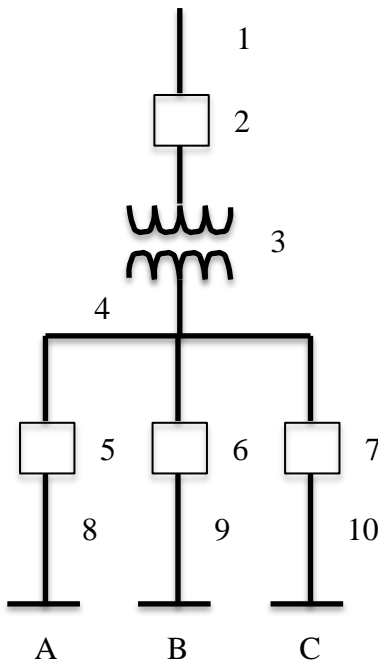


Figure 2.11 Simplified One-Line Diagram of Figure 1.2 Substation

Assume initially that all of the breakers operate properly. At load point A, a failure on feeder 9 will be cleared by opening breaker 6 (as well as feeder 10 failure cleared by breaker 7) so there will be no interruption. Failures of the transmission line (component 1), high-side breaker (component 2), busbar (component 4), feeder breaker (component 5), or feeder (component 8) will result in an outage at load point A equal to the repair time of the respective component. If feeder breaker 6 & 7 fails, high-side breaker 2 will

open, and load point A will experience an outage equal to the time it takes to open the disconnect switches on either side of the breaker and reclose breaker 2 (see Figure 1.2). This switching time would include the time it takes for SCADA to note the breaker operation, a substation crew to be called out to the site, time to troubleshoot the problem, and then perform the isolation.

Generally speaking, components can either fail open or short. Open circuits do not result in breaker operation; short circuits require breaker operation. The total failure rate would therefore be the sum of the open circuit failure rate and the short circuit failure rate. For nearly all substation components, there is practically no open circuit failure mode so open circuits can be ignored. Circuit breakers, on the other hand, can both fail open and short circuit. If feeder breaker 5 in Figure 2.11 fails open, only load point A will experience an outage (equal to the repair time). A short circuit of that same breaker obviously results in the situation previously discussed. These switching actions have been generalized and modeled as active and passive failures (Billinton & Allan, 1996).

2.4.1 Active and Passive Failures

Switching actions in substations can be modeled using a three-state model. The three states illustrated in Figure 2.12 are: (1) the operating or “up” state (U); (2) the switching state in which a component has failed but switching action has not taken place (S); and (3) the repair state in which the fault has been isolated by switching but the repair has yet to begin (R).

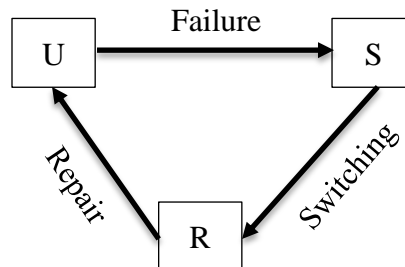


Figure 2.12 Three-State Component Model

For open circuit failures that do not require switching, this reduces to a two-state model as shown in Figure 2.13:

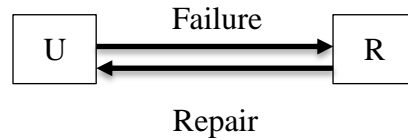


Figure 2.13 Two-State Component Model

Assuming that the repair process is equivalent allows for the models to merge into an equivalent model shown here in Figure 2.14:

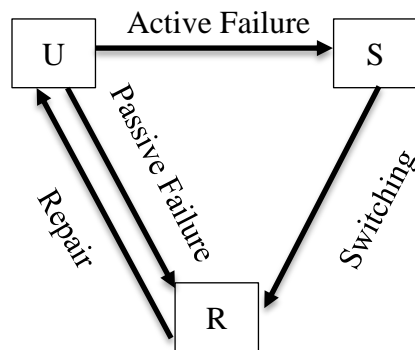


Figure 2.14 Equivalent Component Model

where the failure modes are described as active or passive failure modes. These failure modes are defined (Billinton & Allan, 1996) as:

Passive Failure: “A component failure mode that does not cause operation of protection breakers and therefore does not have an impact on the remaining healthy components.

Service is restored by repairing or replacing the failed component.”

Active Failure: “A component failure mode that causes the operation of the primary protection zone around the failed component and can therefore cause the removal of other healthy components and branches from service. The actively failed component is isolated and the protection breakers are reclosed.” Service is restored to some or all of the load points and the faulted component is repaired or replaced.

The total failure rate would then be the sum of the passive and active failure rate. As discussed previously, for most components the passive failure rate will be zero.

It is also possible for the circuit breakers to malfunction when required to operate. This is known as a “stuck” breaker condition. If there is a fault on the backbone feeder and the breaker fails to clear, the high-side breaker will need to trip to isolate the fault. This stuck breaker condition is different than the active/passive failure mode described previously in that there is an initiating event (e.g., a feeder fault) that calls on the breaker to operate, whereas the active/passive failure modes assume some internal misoperation to the breaker itself. This stuck breaker probability, P_c , can be calculated simply as the proportion of failed operations upon request relative to the total number of operation requests.

2.4.2 Circuit Breaker Operational Failure Modeling

Circuit breakers are required to perform switching actions under fault currents. These switching actions place enormous stress on the breaker components; as such the circuit breaker, and in particular the feeder circuit breakers, will be studied in more detail. The analysis will proceed as follows: (1) a recurrence analysis of operational failures using non-parametric Mean Cumulative Functions (MCFs) will be performed by breaker age; (2) breakers will then be compared by interrupting medium; (3) a parametric model will be fitted by interrupting medium using Maximum Likelihood Estimation (MLE); and finally (4) a prediction of the future number of operational failures will be calculated. This section will provide a background on the methods used and a review of the available technical literature as it applies to circuit breakers. Results of the analyses performed are provided in Section 3.2.2

Heising (1983) presents a summary of failure data presented by industry group and notes some of the issues with reporting breaker failures. Lindquist, Bertling & Erickson (2008) provide average failure rates and fitted Weibull models for high voltage SF₆ (sodium hexafluoride) breaker parts by cumulative number of operations. Bumblauskas et al. (2012) provides a recurrence analysis of breaker warranty claims for SF₆ breakers of varying ages up to twelve years. One of the common themes in all of these references is the difficulty in defining failure, using breaker age or cumulative number of operations in the failure calculation, and the limitations in the data available.

An operational failure will be defined here as an instance where a breaker fails to open or close resulting in corrective action. Breaker age is used in lieu of the arguably better measure of cumulative number of operations as this information is not available.

A repairable system is one in which the system can be restored to operating condition in the event of a failure (Trindade 2006). This does not necessarily mean that the system is “as good as new” as the entire system isn’t being replaced; just that it is capable of being placed back in service through some sort of repair. Repairable systems can be comprised of many repairable or non-repairable components. Non-repairable components are those that either cannot be repaired or that don’t make economic sense to repair. An automobile is a good example of a repairable system in that it is comprised of many components that are either are repaired (batteries recharged) or replaced (tires) and the car then returned to service.

When evaluating a single repairable system, a cumulative plot of the event history (failures, costs, etc.) for that particular system can be plotted versus time or some other more suitable unit such as miles, operations, etc. For non-parametric modeling this is represented by a step function as an example shows in Figure 2.15. Much information is available from these simple types of plots.

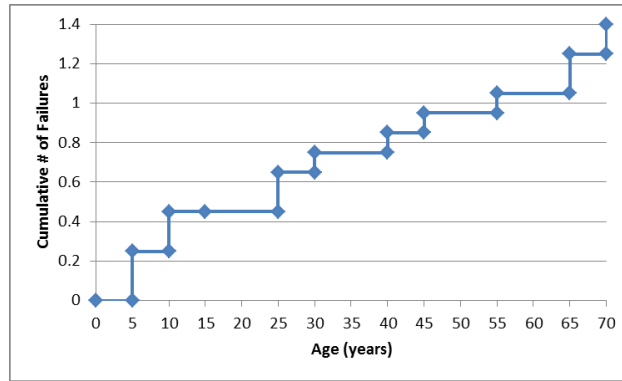


Figure 2.15 Constant Rate of Occurrence of Failure (ROCOF)

The linear plot shown in Figure 2.15 implies that the rate of occurrence of failure (ROCOF), or recurrence rate, is constant with time. This effectively implies that the times between failures, or inter-arrival times, are constant versus time and that the system is neither improving nor deteriorating. Figure 2.16 clearly shows that a system that is deteriorating with time as the slope of the curve increases with time, implying that the time between failures decreases with time. Finally, Figure 2.17 shows a system that is improving with time as the slope of the curve decreases with time, implying that the inter-arrival times are increasing with time.

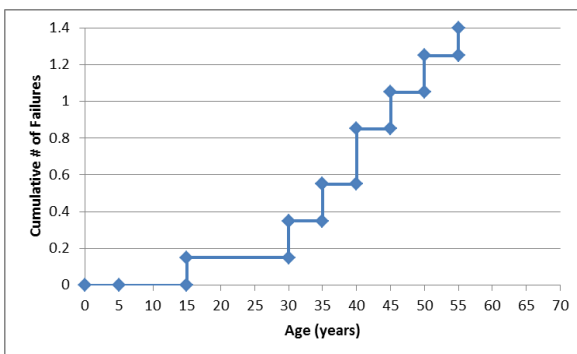


Figure 2.16 Increasing ROCOF

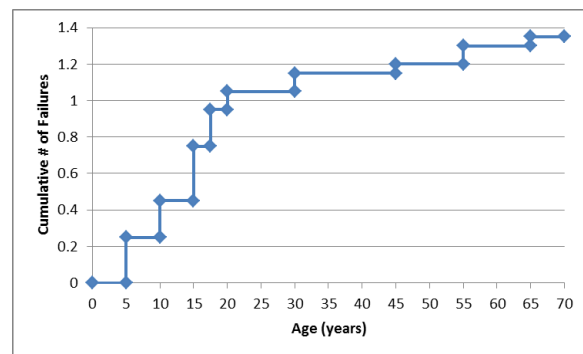


Figure 2.17 Decreasing ROCOF

An important distinction should be made between the recurrence rate of repairable systems and the failure rate of non-repairable systems. In non-repairable systems, the

failure times of individual units are assumed to be independent and identically distributed – that is, the time to failure of the first unit is distributed identically to the second unit and so forth. In repairable systems, this is not necessarily the case as sequential failure times may not be identically distributed – i.e. the sequence of failure matters.

This unit cumulative plot idea can be extended to multiple systems (or a fleet of systems) by developing a Mean Cumulative Function (MCF). The MCF represents the average cumulative performance of all of the systems versus time and is used in lieu of plotting individual cumulative plots for each unit in a fleet of systems. Figure 2.18 below depicts a sample MCF plot:

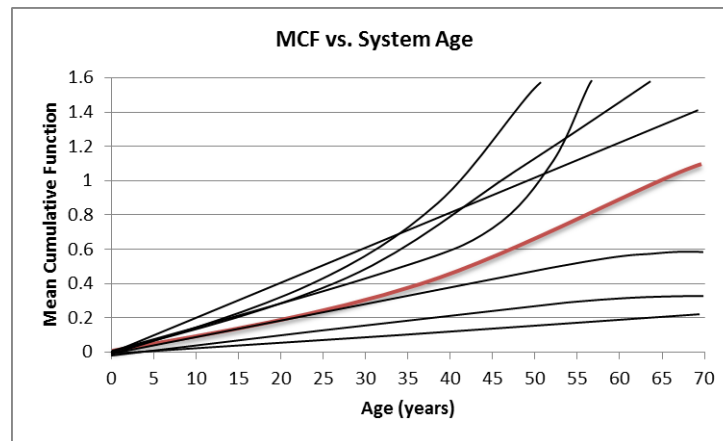


Figure 2.18 Sample Mean Cumulative Function (MCF)

Each of the black lines in Figure 2.18 represents a unit system cumulative plot with the red line representing the MCF for the fleet of all units. This MCF represents the pointwise average of all the individual system cumulative plots with time. In this particular instance, the MCF represents the average cumulative number of failures for all of the units in this system versus time. Alternately, the MCF could represent some other value, such as the mean cumulative repair cost with age; the MCF could also be plotted against some other unit value, such as miles driven, number of operations, etc.

The non-parametric MCF is constructed by increasing incrementally at each failure by taking into account only the units that were in service at that particular time. This method allows for difficult censored and/or truncated data sets, as is the case with staggered entry and limited data availability. Right censoring refers to the instance where event information is not available after a certain unit time – i.e. a circuit breaker that was placed in service and operated for 15 years (and with event information available during the entire 15 years) will not be included in the MCF plot at year 20, simply because the information on the performance of that unit after 15 years is unavailable. This is the case where units were introduced gradually into the field, also known as staggered entry. Similarly, left censoring refers to the instance where the event history of a unit is unavailable prior to a certain age. This typically occurs when data collection begins subsequent to a unit being placed in service. Combinations of left and right censoring can also be addressed in the MCF calculation by appropriately adjusting the number of units in service versus system age.

As an example, a simple MCF is provided here for a fleet of three individual systems (circuit breakers) with only right-censoring. An event plot is shown in Figure 2.19 below with the associated MCF shown in Figure 2.20. In the event plot, the dots denote failure times and the red line termination denotes a right-censoring time. The failures here denote operational failures; the MCF is plotted versus breaker age (in years). The MCF calculation detail is given in Table 2.3.

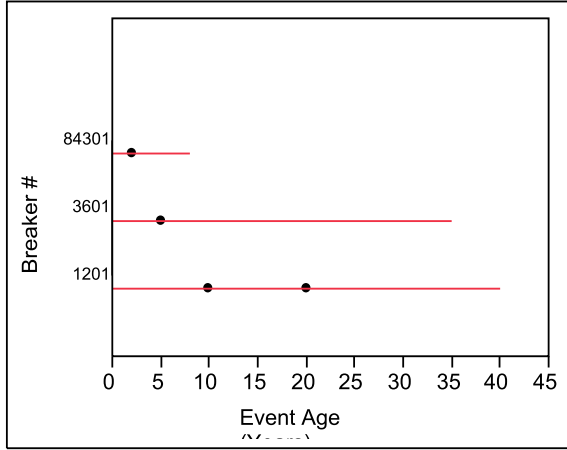


Figure 2.19 Example Event Plot

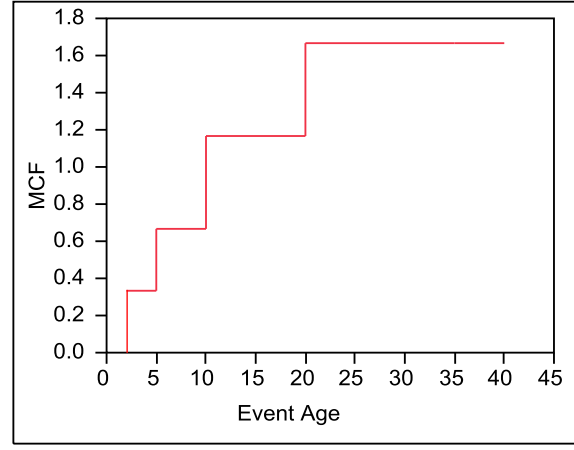


Figure 2.20 Example MCF

Table 2.3 Example MCF Calculation

Event Age (Years)	0	2	5	8	10	20	35	40
Event Description	Start	84301 Failure	3601 Failure	84301 Right Censored	1201 Failure	1201 Failure	3601 Right Censored	1201 Right Censored
Units at Risk	3	3	3	2	2	2	1	0
Failures per unit at Risk	0.000	0.333	0.333		0.500	0.500		
MCF	0.000	0.333	0.667	0.667	1.167	1.667	1.667	1.667

In this simple example, the average number of cumulative operational failures for this fleet of breakers by age 40 is 1.667, and the system is slightly improving with age (intuitively this is unlikely and is strictly a function of the example data).

It is of interest to determine if there is a statistically significant difference in the performance of a particular group relative to others. The methods given in Nelson [2003] and Meeker [1998] allow for pairwise comparisons of the individual mean cumulative functions as follows:

$$\Delta(t) = MCF_1(t) - MCF_2(t)$$

$$Var[\Delta(t)] = Var[MCF_1(t)] + Var[MCF_2(t)]$$

$$\text{with associated } se_{\Delta} = \sqrt{Var[\Delta(t)]}$$

so a 95% confidence interval for the difference in the grouped MCFs is as follows:

$$[\underline{\Delta}(t), \bar{\Delta}(t)] = [\Delta(t) - z_{0.975} se_{\Delta}, \Delta(t) + z_{0.975} se_{\Delta}]$$

These are pointwise confidence limits and only apply to a single instance in time versus a simultaneous interval which would apply to the interval MCF difference. If the limits of the interval do not enclose zero for a significant portion under study then there is a statistically significant difference between the two groups under observation.

It is also of interest to have an idea of the expected number of future operational failures. To do so, a parametric model must be fitted to the data; previous sections have dealt with non-parametric estimates of the MCF. Generally, if a MCF has a constant recurrence rate then it can be modeled with a Homogeneous Poisson Process (HPP), where the recurrence rate is λ and the expected number of recurrences over time Δt is $\lambda\Delta t$.

If, however, the recurrence rate is not constant, a Non-Homogeneous Poisson Process (NHPP) can be fitted to the data. There are a couple of different NHPP model options available, but for this analysis the NHPP Power Process is used, where:

$$M(t) = \alpha t^\beta$$

where the beta and alpha parameters are fitted to the data using Maximum Likelihood Estimation (MLE). If beta is less than one, the recurrence rate decreases with time signifying a system that improves with time; for beta = 1 the recurrence rate is constant and the model reduces to the HPP (the HPP is therefore shown to be a special case of the NHPP); if beta is greater than one then the recurrence rate increases with time and the system is deteriorating. The recurrence rate can be calculated as:

$$\lambda(t) = \frac{d[M(t)]}{dt} = \alpha\beta t^{\beta-1}$$

The Maximum Likelihood estimates for the NHPP Power model are given in Crow (1975) as follows:

$$\hat{\alpha} = \frac{\sum_{q=1}^K N_q}{\sum_{q=1}^K (T_q^{\hat{\beta}} - S_q^{\hat{\beta}})}$$

$$\hat{\beta} = \frac{\sum_{q=1}^K N_q}{\hat{\alpha} \sum_{q=1}^K (T_q^{\hat{\beta}} \ln T_q - S_q^{\hat{\beta}} \ln S_q) - \sum_{q=1}^K \sum_{i=1}^{N_q} \ln X_{i_q}}$$

where:

K = # of systems under study

q = current system, q = 1, 2,..., K

S_q = observation start time for system q

T_q = observation termination time for system q

N_q = # of failures experienced by the q-th system

X_{iq} = age of system q at the ith occurrence of failure, i = 1, 2,..., N_q

The number of expected occurrences in the interval (t₁, t₂) can be calculated as follows:

$$N(t_1, t_2) = \int_{t_1}^{t_2} \lambda(t) dt = \int_{t_1}^{t_2} \alpha \beta t^{\beta-1} dt$$

We are interested in the expected number of future failures given the current age of the individual units in service. As an example, let's assume that we have fitted the NHPP Power Process Model via MLE with fitted parameters alpha = 0.0029 and beta = 1.2575 (beta > 1, implying an increasing recurrence rate). Let's also say that we are interested in breakers that are 47 years old and assume that there are currently 25 units of this age in service. The total cumulative expected number of future failures in the next five years is therefore as follows:

$$N_{47}(52, 47) = \int_{47}^{52} (1.2575)(0.0029)t^{1.2575-1} dt$$

$$N_{47}(52, 47) = 0.019797 \text{ failures per unit at risk}$$

$$(0.019797)(25) = 1.2449 \text{ failures}$$

So the contribution to the total cumulative number of future failures is 1.25 failures. The total cumulative expected number of future failures would then be the sum of the individual contributions from each breaker interval.

2.4.3 Substation Failure Mode and Effects Analysis

It is now possible to apply the active and passive failure modeling to the substation FMEA. Billinton & Allan (1996) provide an algorithm for the evaluation of the failure modes at each load point as follows

1. Evaluate minimum cut sets simulating total failure events
2. Evaluate minimum cut sets simulating active failure events and stuck breakers as follows:
 - a. Select a component to simulate the active failure.
 - b. Determine if the active failure of the selected component and/or its protective breakers appears between the load point being studied and a source. If not, ignore.
 - c. If these components break all source paths, this active failure is a first-order failure event.
 - d. If these components break only some of the source paths, evaluate the minimum cuts sets of the remaining source paths. These represent second-order or higher failure events.
 - e. Determine if cut sets are already contained in a lower order failure event; if so discard.
 - f. Repeat for all remaining components.

Using the algorithm above for the sample substation shown in Figure 2.11, the failure events at load point A are therefore:

Total Failure Events: {1}, {2}, {3}, {4}, {5},{8}

First-Order Active Events: {6A}, {7A}

Second-Order Active Events: {9A & 6S}, {10A & 7S}

The failure rate and repair times for these first and second order events is calculated as follows:

First-Order Event (Component 1 active failure):

$$\lambda_a = \lambda_1^a$$

$$r_a = s_1$$

where s_1 is the switching time of component 1.

Second-Order Event (Component 1 active failure and Component 2 Total Failure)

$$\lambda_a = \lambda_1^a \lambda_2 (s_1 + r_2)$$

$$r_a = \frac{s_1 r_2}{s_1 + r_2}$$

Stuck Breaker

$$\lambda_a = (\lambda_1^a) P_c$$

$$r_a = s_b$$

where s_b is the time to switch the breaker.

As an example, the reliability of the substation in Figure 2.11 can now be evaluated using the assumed component values given in Table 2.4:

Table 2.4 Component Data for Substation in Figure 2.11

Component	λ (f/yr)	λ^a (f/yr)	r (hrs)	s (hrs)	P_c
T-Line 1	0.09	0.09	9	-	-
H.V. Breaker 2	0.02	0.01	5	-	0.05
Xfmr 2	0.05	0.05	24	-	-
Bus 4	0.01	0.01	3	-	-
L.V. Breaker 5, 6,7	0.02	0.01	5	2	0.05
Feeder 8, 9, 10	0.01	0.01	2	2	-

Using the values in Table 2.4, the reliability indices for load point A can be calculated as follows in Table 2.5:

Table 2.5 System Reliability of Load Point A in Figure 2.11

Min Cut Set	λ (f/yr)	r (hrs)	U (hrs/yr)
1	0.09	9	0.81
2	0.02	5	0.10
3	0.05	24	1.20
4	0.01	3	0.03
5	0.02	5	0.10
8	0.01	2	0.02
6A	0.01	2	0.02
7A	0.01	2	0.02
9A+6S	0.0005	2	0.001
10A+7S	0.0005	2	0.001
Total	0.221	10.413	2.302

2.5 Distribution System Assessment

Consider the feeder shown in Feeder 2.21, which represents Feeder #1 to be used in forthcoming sections. There are seven (7) load points representing various customer types (residential/commercial/industrial) with the number of customers shown.

Residential customers are fed from 1-Ø lines; commercial and industrial customers are fed from 3-Ø lines. These load points are located behind fused taps off of the main backbone feeder in order to isolate faults. The feeder exits the substation underground (denoted by the dotted lines), typically in a concrete-encased ductline. The underground cables rise up on wooden poles and form the main backbone. There are three (3) normally closed sectionalizing switches (S1, S2, S3) that are used to isolate faulted feeder sections. A normally open tie switch (S4) allows for load transfers to the adjacent feeder.

As an example, assume that a fault has occurred on Section 4 in Figure 2.21. The feeder breaker at the substation opens and all customers on that feeder experience an outage. A troubleshooter is dispatched to locate the fault. After finding the fault, the

troubleshooter will open switch S1 and S2, SCADA will close the feeder breaker back thereby restoring power to customers at load points 1 & 2. The troubleshooter then closes the normally open tie switch and power is restored to the customers at load points 5, 6 & 7. A repair crew is called out to repair the faulted portion of section 4, meaning that all of the customers at load points 3 & 4 will experience an outage equal to the repair duration and the time required to reconfigure the system back to its original state.

The addition of fuses on lateral taps changes the sections of the feeder that contribute to failures at each respective load point. If the load point of interest is load point #2 in Figure 2.21, a fault somewhere along section #2 will cause the fuses to isolate that fault, assuming the fuse operates properly. If the fuse does not operate properly, the failure rate contribution of the faulted section can be calculated as follows (Billinton & Allan, 1996):

$$\text{Failure Rate} = (\text{Failure Rate}|\text{Fuse Operates}) * P(\text{Fuse Operates}) + (\text{Failure Rate}|\text{Fuse Fails}) * P(\text{Fuse Fails})$$

The addition of sectionalizing and tie switches along the feeder can reduce the outage duration experienced. It should be noted, however, that the addition of these switches does not reduce the frequency of interruptions as any fault along the backbone will cause the breaker to trip. If there are no capacity concerns associated with transferring load then the outage duration of the load points on the switchable sections is simply the time associated with the switching operation. If there are capacity concerns, and the probability of transfer is known, the expected outage duration of the appropriate switchable section can be calculated as follows (Billinton & Allan, 1996)

$$\text{Outage Time} = (\text{Outage Time}|\text{Fuse Operates}) * P(\text{Transfer}) + (\text{Outage Time}|\text{No Transfer}) * P(\text{No Transfer})$$

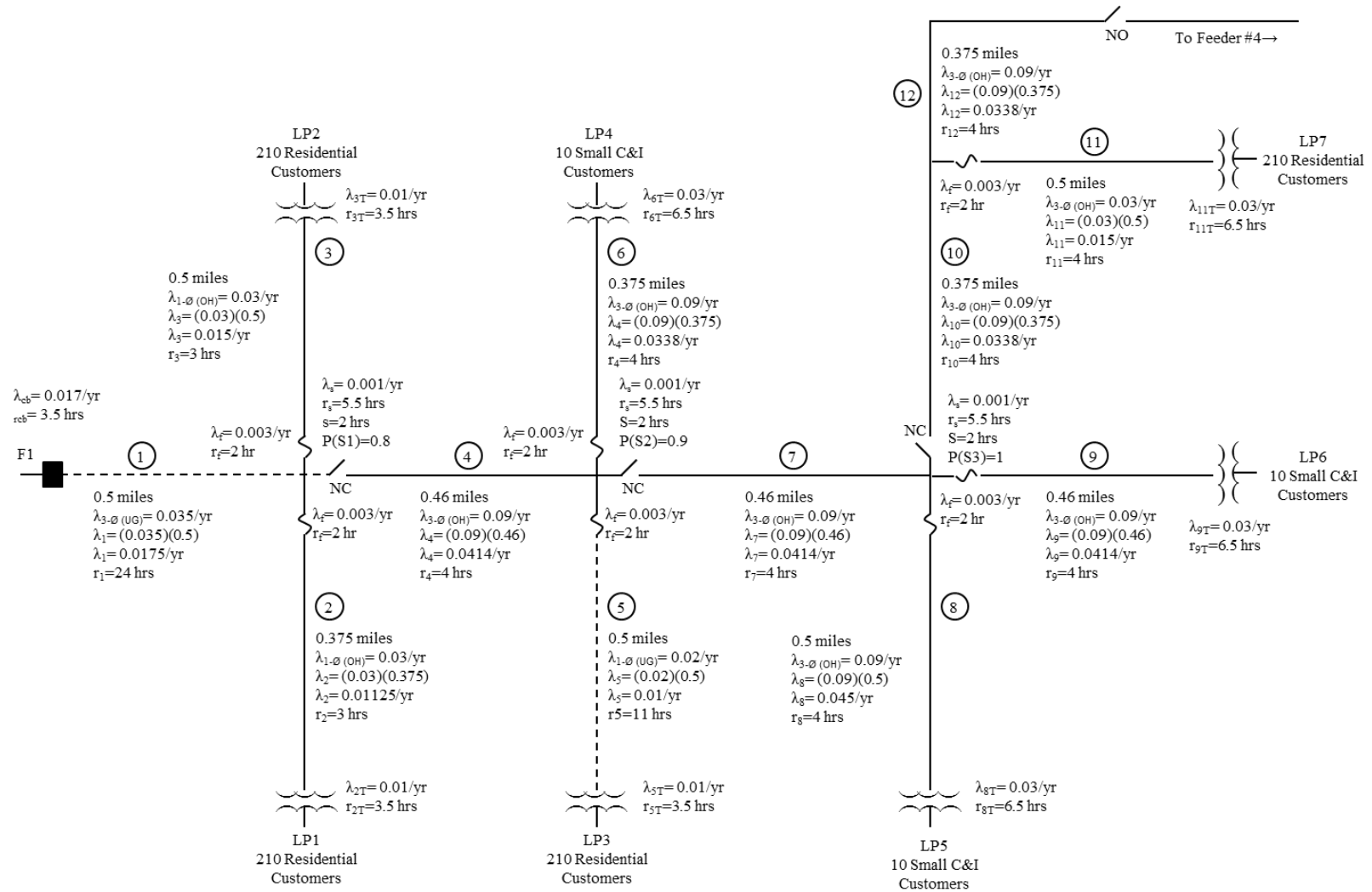


Figure 2.21 Feeder #1

As an example of these ideas in application with the series systems equations, the reliability indices as calculated for load point #3 in Figure 2.X are as follows:

$$\begin{aligned}\lambda_{LP\#3} &= \lambda_{CB} + \lambda_1 + \lambda_2\lambda_{2F} + \lambda_3\lambda_{3F} + \lambda_{S1} + \lambda_4 + \lambda_5 + \lambda_{5F} + \lambda_{5T} + \lambda_{S2} + \lambda_7 + \lambda_8\lambda_{8F} + \\ &\quad \lambda_9\lambda_{9F} + \lambda_{S3} + \lambda_{10} + \lambda_{11}\lambda_{11F} + \lambda_{12} \\ \lambda_{LP\#3} &= 0.2114 \text{ f / yr} \\ U_{LP\#3} &= [(s_{S1})(P_{S1}) + (r_{CB})(1 - P_{S1})]\lambda_{CB} + [(s_{S1})(P_{S1}) + (r_1)(1 - P_{S1})]\lambda_1 + \\ &\quad [(s_{S1})(P_{S1}) + (r_{2F})(1 - P_{S1})]\lambda_2\lambda_{2F} + [(s_{S1})(P_{S1}) + (r_{3F})(1 - P_{S1})]\lambda_3\lambda_{3F} + \\ &\quad \lambda_{S1}r_{S1} + \lambda_4r_4 + \lambda_{5F}r_{5F} + \lambda_5r_5 + \lambda_{5T}r_{5T} + \lambda_6\lambda_{6F}r_{6F} + \lambda_{S2}r_{S2} + \lambda_7s_{S2} + \lambda_8\lambda_{8F}s_{S2} + \\ &\quad \lambda_9\lambda_{9F}s_{S2} + \lambda_{S3}s_{S2} + \lambda_{10}s_{S3} + \lambda_{11}\lambda_{11F}s_{S3} + \lambda_{12}s_{S3} \\ U_{LP\#3} &= 0.69947 \text{ hrs / yr} \\ r_{LP\#3} &= \frac{U_{LP\#3}}{\lambda_{LP\#3}} = \frac{0.69947 \text{ hrs / yr}}{0.2114 / \text{ yr}} = 3.309 \text{ hrs}\end{aligned}$$

2.6 Decoupled Composite Model Assessment

Traditionally, the calculation of reliability impacts has been handled separately for the transmission, substation, and distribution systems. Technical literature generally focuses on the analysis of a particular subsystem. Commercially available software is able to calculate distribution system reliability values but ignores the substation and transmission system impacts. Brown and Taylor (1999) provide a method for evaluating the reliability impacts of the substation and transmission systems on the distribution system through the use of decoupled composite modeling. Essentially, the outputs of the various subsystem reliability assessments are used as an equivalent input in the distribution system analysis. The equivalent expected outage frequency, repair time, and outage duration for the transmission and substations are then modeled as an equivalent block in series with the distribution system components. The system is then easily evaluated using the methods described in previous sections.

2.7 Reliability Benefit-Cost Analysis

The methods described in previous sections allow for the development of a predictive reliability model of a power system. This model can then be used to estimate the impacts of various projects aimed at improving the reliability of the system. Each

utility will have to decide how to define reliability, whether via SAIFI, SAIDI, customer outage costs, etc. Choudhury & Koval (2009) and Brown (2000) provide valuable options for using a benefit-cost approach to reliability-based planning with the former using both the reliability indices, customer outage costs, and a cost/kW as bases for benefit calculation, whereas the latter introduces the concept of marginal cost-benefit planning whereby multiple project options for the same project are introduced and benefits are maximized at the expense of cost, minimum BCR, and marginal BCR constraints.

This thesis will use CMI as the benefit when comparing project options, with the benefit-cost of a project option simply being the project costs divided by the change in CMI relative to some base case. A group of projects can then be ranked in order of decreasing \$/CMI spent, where \$/CMI is used to compare the efficiency of each reliability dollar spent. These projects can then be plotted without interaction cumulatively and the utility can then choose an appropriate budget amount to maximize reliability.

CHAPTER 3

COMPOSITE POWER SYSTEM RELIABILITY EVALUATION

The model used in this thesis is a hybrid of actual 161 kV transmission lines feeding a 161-23 kV substation from a utility located in the Southeast United States. The substation has been modified slightly at the feeder breaker level so as to work with a four feeder distribution test system (Allan et al., 1991). The distribution system itself has been modified to assist in comparing projects across work areas.

3.1 Transmission Reliability Evaluation

The existing transmission line route is shown in red in Figures 3.1. As denoted in the figure, there is a section of the existing transmission feed that shares common structures. The loss of a single structure in this common-tower section due to some external event, such as a vehicle impact, could result in complete substation outage. It should be noted that there is also the potential for a single external event to outage multiple structures sharing a common-Right-Of-Way (ROW). For example, a wildfire, flood, or tornado in the area could likely outage multiple structures sharing a common-ROW. The forthcoming analysis will not quantify these potential impacts and it will not be addressed further.

The lengths of the transmission circuits feeding the substation and the respective common-tower exposed lengths are given in Table 3.1.

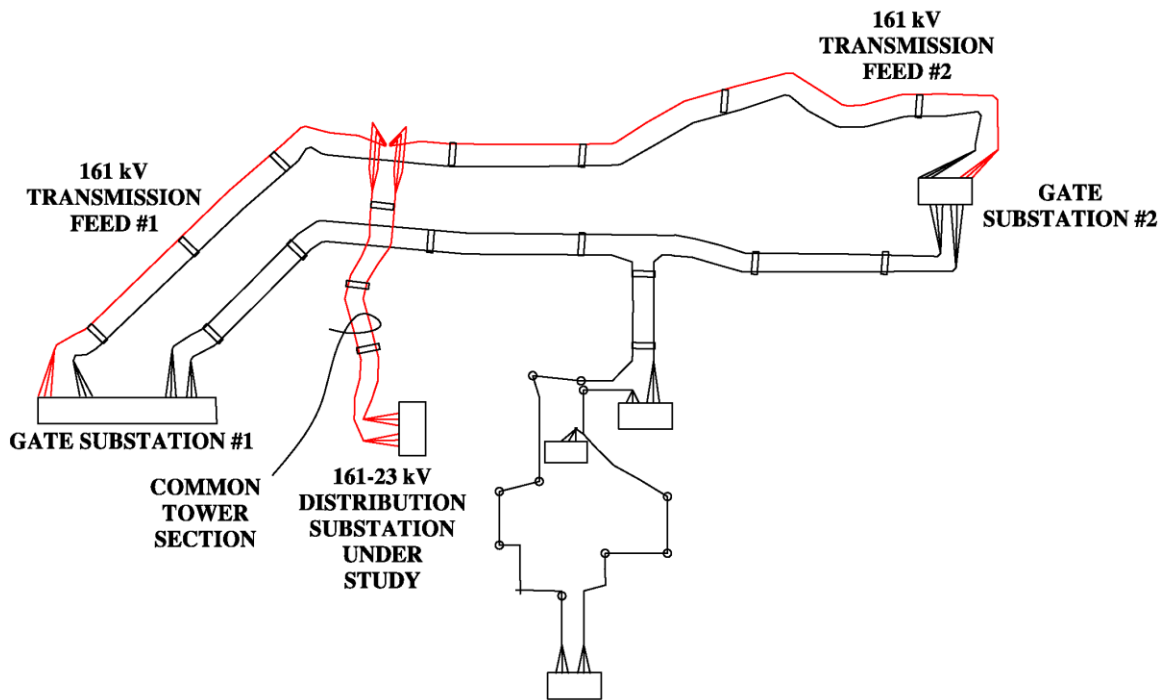


Figure 3.1 Existing Transmission Route

Table 3.1 Transmission Circuit Lengths

Circuit	Length (ft)
Feed #1	21,265
Feed #2	37,517
Common-Tower	8,627

Failure rates and repair times must be known to use the models. Oklahoma Gas and Electric Company's experience (Masud 1976), exclusive of lightning, is reproduced here in Table 3.2:

Table 3.2 Transmission Line Data

Line Voltage (kV)	Failure Rate (outages/mile-year) λ	Repair Duration (hours) r
69	0.011	6
138	0.0065	9
161	0.0050	9
345	0.0025	12
500	0.0020	12

Only one source (Landgren et al., 1986) presents specific information on common-tower outage rates. This information, however, is for 345 kV transmission lines and for differing design years and exposure. In most technical references the common-mode failure rate is assumed to be a proportion of the independent failure rate (i.e. λ_c/λ). In the discussion of Billinton et al. (1981), Commonwealth Edison's experience is that the common-cause failure mode is between 15%-18% of the independent rate. A range of values will be plotted in this analysis, with the detailed comparison presented at a value of 20%.

Applying the model shown in Figure 2.11 with the line lengths in Table 3.1 and the outage data in Table 3.2 results in the steady-state probability of being in State 4 (both circuits down) as shown in Figure 3.2 for various values of λ_c/λ :

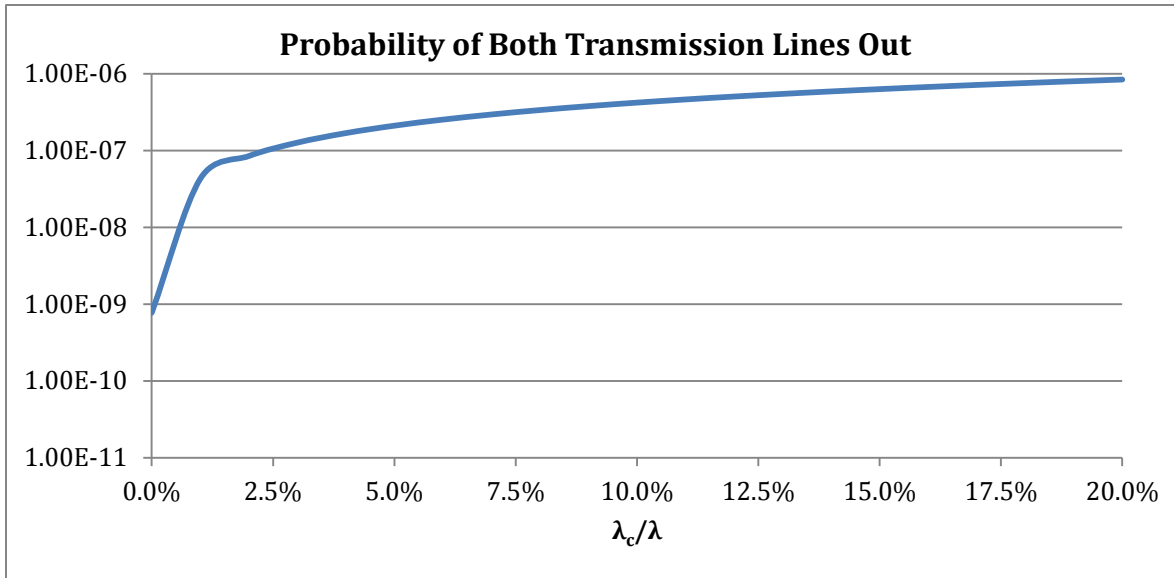


Figure 3.2 State 4 Probabilities for Substation Transmission Feed

This plot shows that the steady-state probability of both lines being down is exceedingly low. It should first be pointed out that including a common-cause failure mode increases the steady-state probability of State 4 by several orders of magnitude. This implies that not including this failure mode would result in more optimistic results. It also appears that the increase in the ratio of λ_c/λ slowly changes the steady-state probabilities after about 2.5%.

At $\lambda_c/\lambda = 20\%$, the steady-state probability of both lines down is 8.37×10^{-7} . This value can be interpreted as the proportion of time this arrangement is expected to spend in this state. Since the lines are in a parallel arrangement, we can sum the steady-state probabilities of States 1, 2 & 3 to find that we expect to find at least one of the lines up 99.9999163% of the time.

The expected average annual unavailability (U) of the transmission feed to Substation 49 for the expected and proposed cases can therefore be calculated as:

$$U_{\text{existing}} = (8.37 \times 10^{-7})(8760 \text{ hrs/yr}) = 0.0073 \text{ hrs/yr}$$

3.2 Substation Reliability Evaluation

Substation reliability indices will now be evaluated using the methods presented in Section 2. The substation model will be presented first. A circuit breaker operational failure recurrence analysis will follow with the remaining component modeling coming thereafter. Cut sets in concert with the component data will inform the FMEA calculation and associated substation reliability indices.

3.2.1 Substation Model

The substation one-line diagram is shown in Figure 3.3. The two (2) 161 kV transmission feeds are shown with a normally closed high side breaker (breaker 8). These then feed two (2) 161-23 kV power transformers that in turn feed a 23 kV operating bus split by a normally open sectionalizing breaker (breaker 7). The four feeders of the distribution system tap off of the operating bus. The switches shown are non-load break switches meant to serve as visible confirmation of open/closed circuits. Circuit breaker component modeling will be presented in the next section with the remaining component information following thereafter. This information will then be used with the cut sets to calculate the reliability indices in the final substation evaluation section.

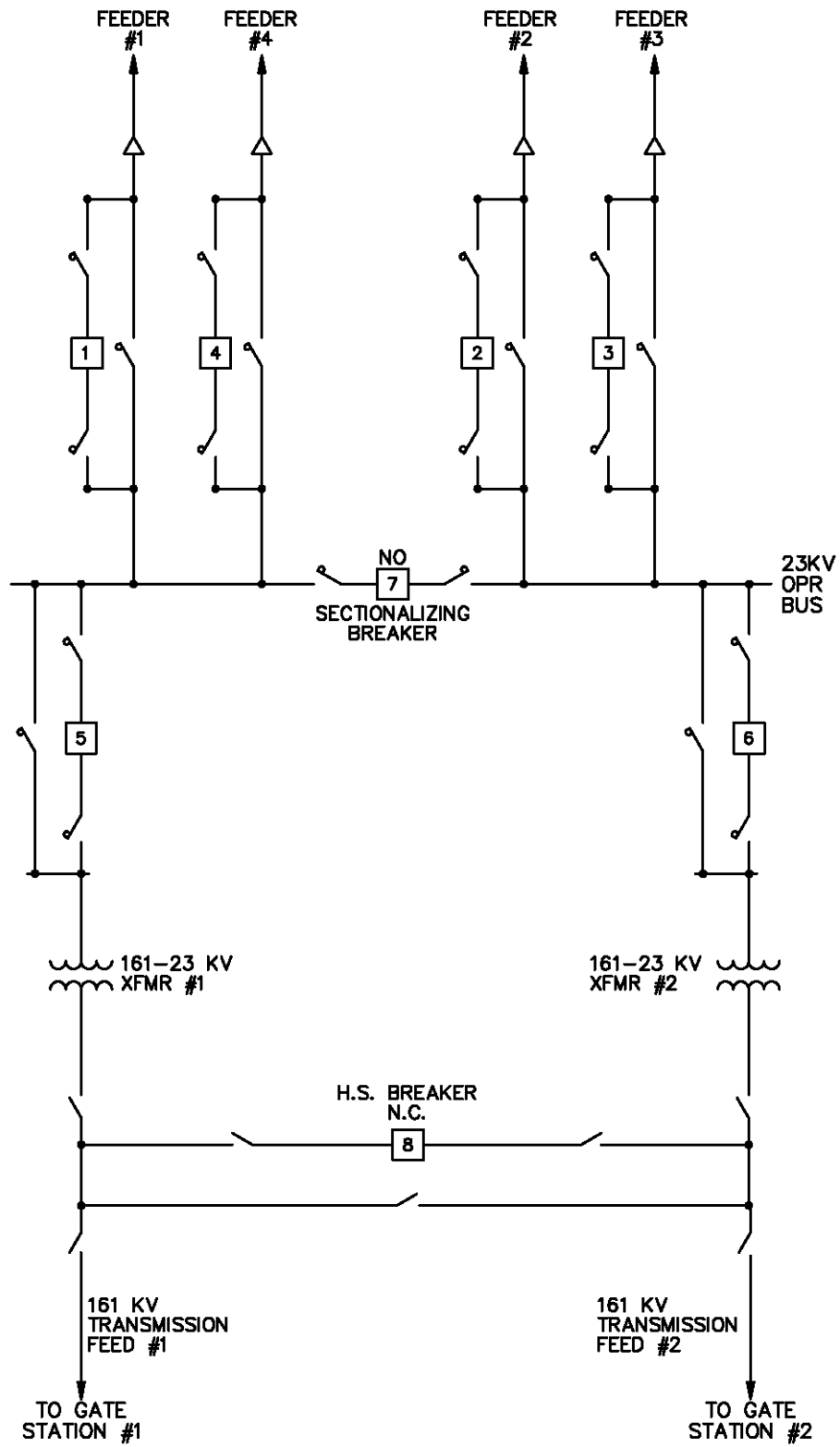


Figure 3.3 Substation One-Line Diagram

3.2.2 Circuit Breaker Operational Failure Recurrence Analysis

There are approximately 495 substation feeder circuit breakers currently operating at 12 or 23 kV at a utility in the Southeast United States that form the dataset for this analysis. The median breaker age, regardless of interrupting medium, is 36 years. Oil-interrupting breakers represent the majority of these (64%; median age 43 years) with the remainder roughly evenly distributed between SF₆ gas-interrupting breakers (18%; median age 21 years) and vacuum-interrupting breakers (18%; median age 11 years). Since 1993, there have been approximately 126 operational failures attributed to these feeder circuit breakers; an operational failure is defined as an instance where a breaker fails to open/close resulting in corrective action. These operational failures have resulted in lengthy customer outages and repair times.

A complete listing of breakers under study and associated details is provided in a supplemental file to this thesis (File 2, feeder_summary.xls). Operational failure historical data is available from 1993-present; a breakdown of breaker age and interrupting medium is provided in Figure 3.4 & 3.5. As is shown, there is a considerable amount of operational failure information that is not available for study resulting in heavily left-censored data – particularly for the oil breakers.

Several important assumptions have been made. The first is that if the age of the breaker is not explicitly provided in the breaker dataset, it is assumed to have been placed in service at the date the substation was energized. The second is that only events resulting in outage times greater than 5 minutes are included in the operational failure listing. This is to remove instances of breaker operations due to lightning, clear temporary faults, etc., and to focus on events that impact reliability indices. It also excludes any maintenance activity that did not result in an outage to customers. This analysis also only focuses on distribution feeder breakers – high side breakers, capacitor bank breakers, tie breakers, etc., are excluded from study.

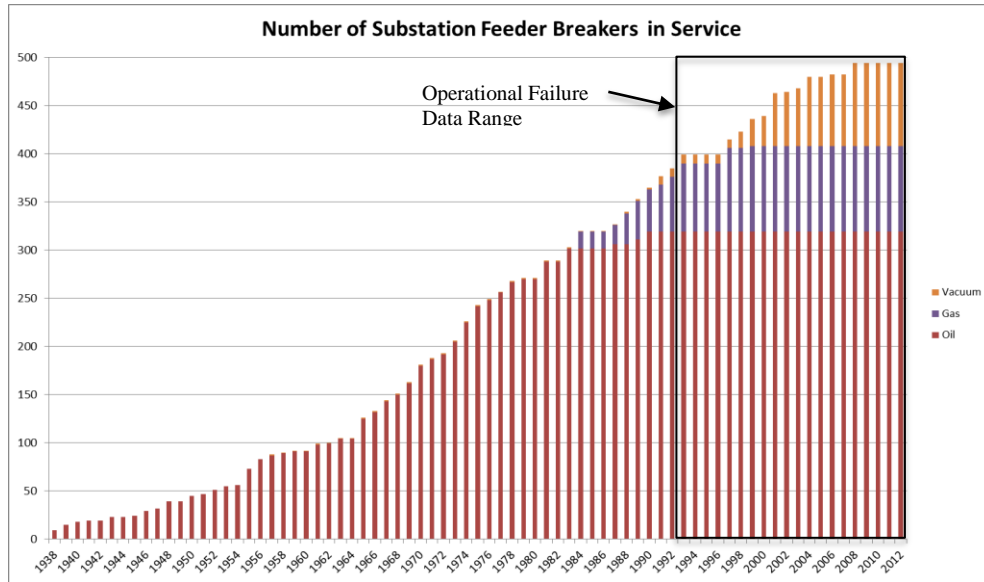


Figure 3.4 Feeder Breakers In Service

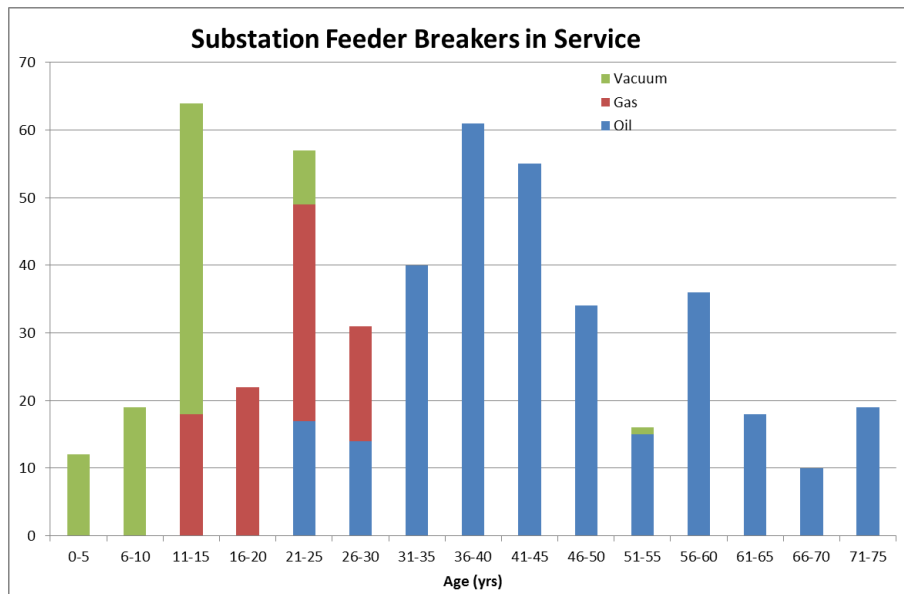


Figure 3.5 Feeder Breakers by Age

It was necessary to shift the data from calendar time to event time, as shown in the representative event plots for the breakers given below. In Figure 3.6, the breaker

information for the breakers in calendar time; Figure 3.7 shows the data adjusted to a common starting time to allow for MCF calculation.

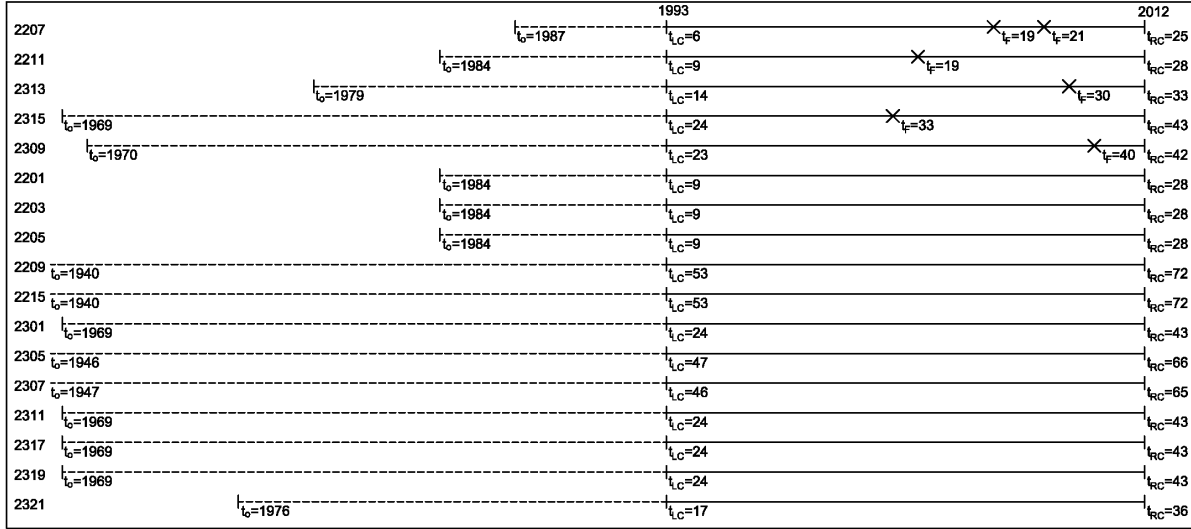


Figure 3.6 Breaker Event Plot by Calendar

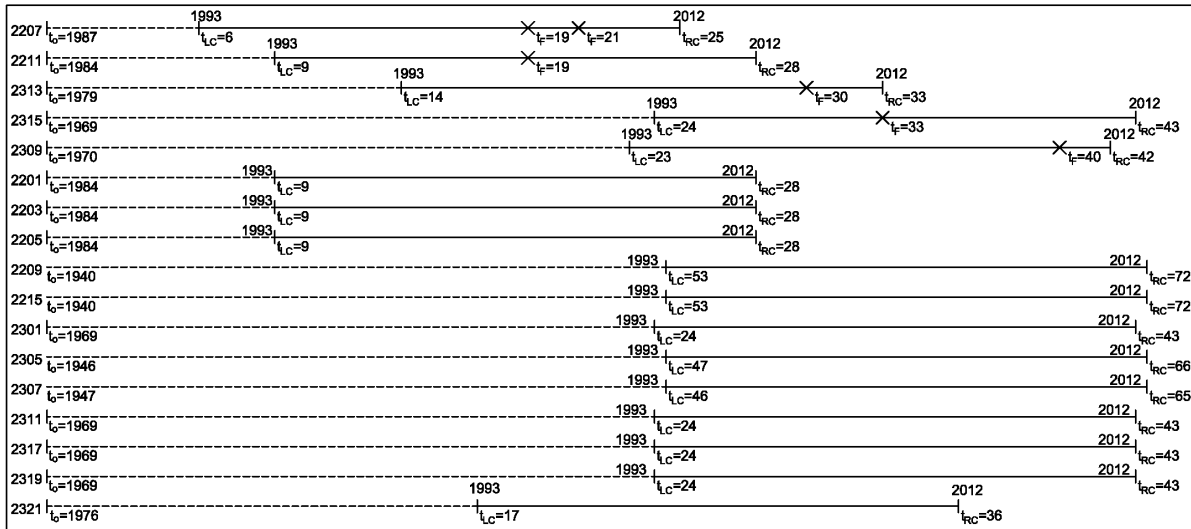


Figure 3.7 Shifted Breaker Event Plot

There were several instances of operational failures that had to be excluded from consideration as these failures occurred prior to the installation of the current breaker in the database and no information on the replaced breaker was available. These values would have resulted in negative event times.

Operational failure modes, when provided or ascertained, are summarized in Figure 3.8. As can be seen, the majority of the failure causes are either unknown or were not input into the reliability database. When provided, the dominant failure mode is low pressure resulting in nearly 30% of all failures.

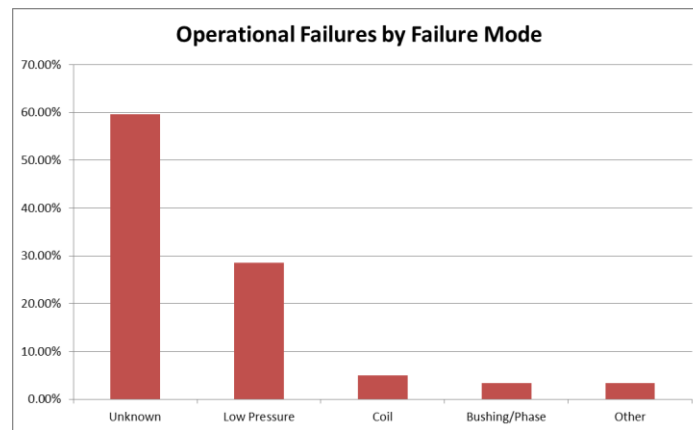


Figure 3.8 Failure Modes

The low pressure failure mode is exclusive to oil and gas breakers. In the case of the oil breakers, the closing operation is based on a hydraulic actuating mechanism driven by a 90-220 psi tank, compressor, and motor assembly. Generally, this assembly can perform three operations without recharging. The tripping operation is performed separately by a spring and operates independently of this hydraulic system. Gas breakers are filled with SF₆ gas and are unable to open or close when gas leaks out through O-rings. A closer investigation of the failure data reveals that the breakers fail open approximately 90% of the time.

The methodology described in previous sections was applied to the breaker data with the aforementioned assumptions. Due to the complicated censoring, the interval-age approach given in Nelson (2003) was extended to include left-censored data and used in the analysis. It should be noted that, at present, commercially available statistical analysis packages (JMP, etc.) do not allow for left censoring in recurrence platforms so all of the analysis was performed via Excel spreadsheets. Initially, all of the breakers are considered together and a “system-of-systems” MCF is plotted. This MCF is informative but does not necessarily reveal underlying trends that can potentially motivate action. As such, the data are then sorted by interrupting medium and MCFs are then calculated for each and compared. Due to the limitations of the data (small samples sizes, no failures, etc.), it is not feasible to create MCFs by breaker manufacturer.

All of the breakers are initially aggregated to create a pooled MCF for the entire feeder breaker fleet. Figure 3.9 shows this system MCF with associated 95% confidence interval bands. The censored units are assumed to have either entered or exited halfway through the interval on average (done by multiplying units at risk by 0.5). This step extends the methodology given in Nelson (2003) to account for the left-censored observations. A supplemental file to this thesis (File 3, system_mcf.xls) displays the MCF calculation and associated confidence interval widths.

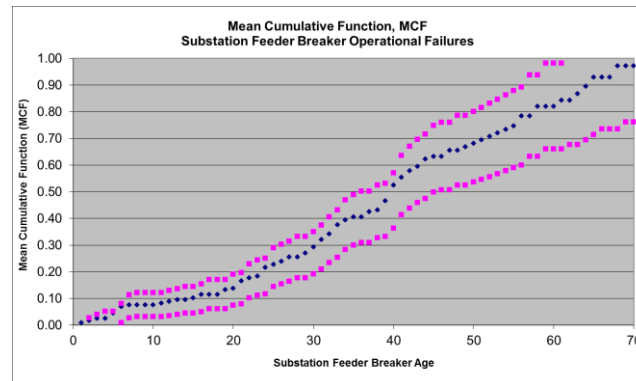


Figure 3.9 Pooled MCF

It is apparent from the system MCF that the system is deteriorating with time as the MCF slope is increasing. Intuitively this makes sense due to aging components. The breaker data were then sorted by interrupting medium and grouped MCFs plotted with associated 95% confidence intervals as shown in Figures 3.10 thru 3.12.

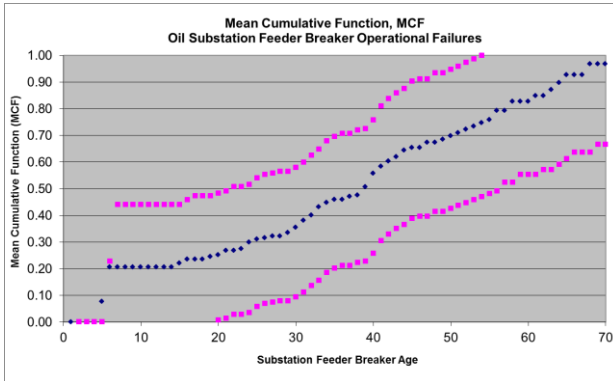


Figure 3.10 Non-Parametric Oil MCF

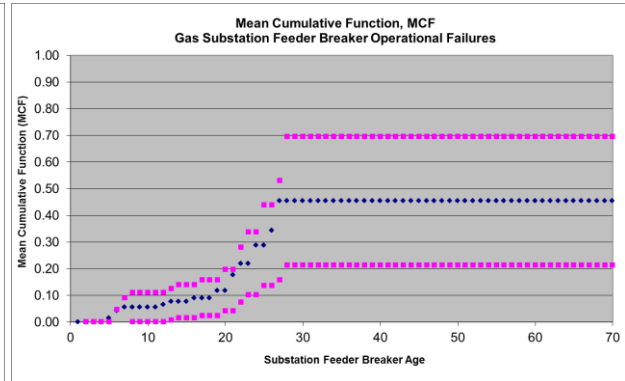


Figure 3.11 Non-Parametric Gas MCF

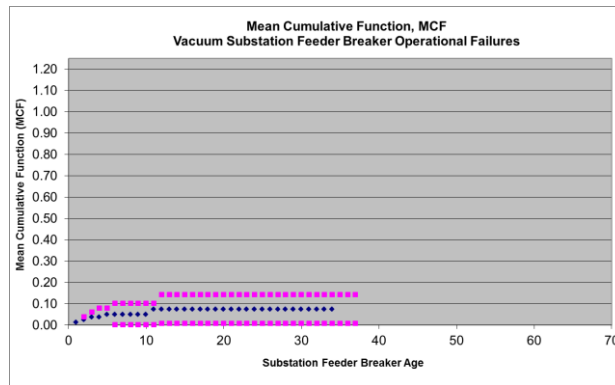


Figure 3.12 Non-Parametric Vacuum MCF

The oil breaker MCF shown Figure 3.10 has the largest range of data; the confidence interval half-width is large due to the small number of early age units at risk and the fact that the variance is additive with time. The left-censoring from the operational failure data unavailability is ultimately a non-issue as the performance of the oil breakers early in life is non-informative – i.e., a breaker that fails catastrophically and is replaced will not be replaced with an oil breaker. A supplemental file to this thesis (File 4, oil_mcf.xls) displays the calculation details.

The gas breaker MCF shown in Figure 3.11 clearly shows a deteriorating system as the recurrence rate is increasing with system age. For convenience of comparison the MCF is plotted through 70 years though it is non-informative after ~30 years due to the range of the data. Obviously, the gas breakers are a cause for concern. A supplemental file to this thesis (File 5, gas_mcf.xls) displays the calculation details.

The vacuum breaker MCF is plotted in Figure 3.12 and shows a recurrence rate that is roughly constant with time. Again, the MCF is plotted through 70 years for convenience but should be ignored after ~38 years due to the data range. Clearly the performance of the vacuum breakers is superior to that of the oil and gas breakers. A supplemental file to this thesis (File 6, vacuum_mcf.xls) displays the calculation details.

Figure 3.13 plots the difference in the MCF's between the gas and vacuum breakers:

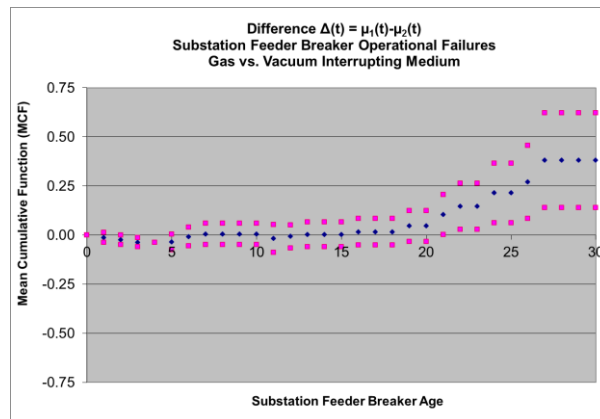


Figure 3.13 Gas vs. Vacuum Breakers

As can be seen above, the pointwise confidence limits do not envelop zero for the range of the data after roughly 20 years so there is a statistically significant difference between the gas and vacuum breakers at the level of significance chosen. Due to the heavy left-censoring of the oil breakers relative to the range of the data for the gas and vacuum breakers, it is not feasible to compare the oil breakers.

The results of the parameter estimation for each of the breaker types using the MLE methods in section 2.4.2 are given in Table 3.3. Based upon the visual trend tests and the fitted beta values, it is assumed that the vacuum breakers follow the HPP process and the gas breakers follow the NHPP model. Given the uncertainty due to small sample sizes for oil breakers less than age ~20, a formal determination of HPP/NHPP will not be made

Table 3.3 MLE Fitted NHPP Model Parameters

Breaker Type	$\hat{\alpha}$	$\hat{\beta}$
Oil Interrupting	0.003659	1.3319
Gas Interrupting	0.000136	2.3877
Vacuum Interrupting	0.0063	1.0

Figures 3.14 thru 3.15 show the non-parametric estimates as well as the fitted parametric models; Figure 3.17 plots the recurrence rate for each of the fitted models.

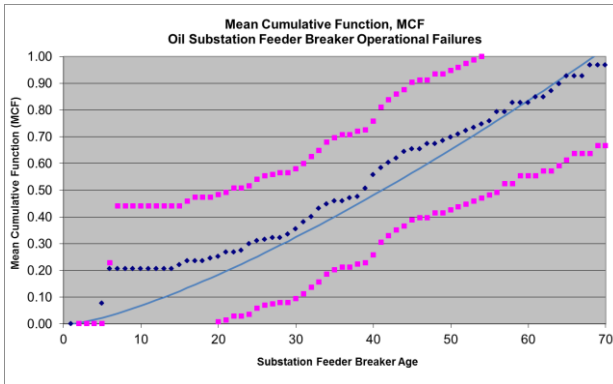


Figure 3.14 Fitted Oil MCF

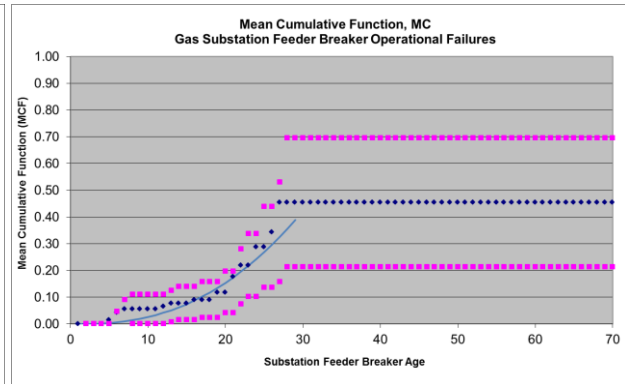


Figure 3.15 Fitted Gas MCF

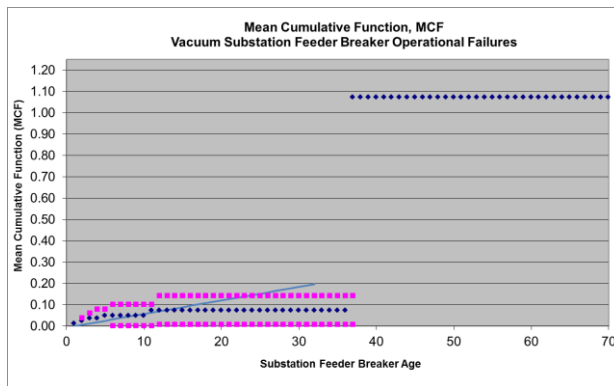


Figure 3.16 Fitted Vacuum MCF

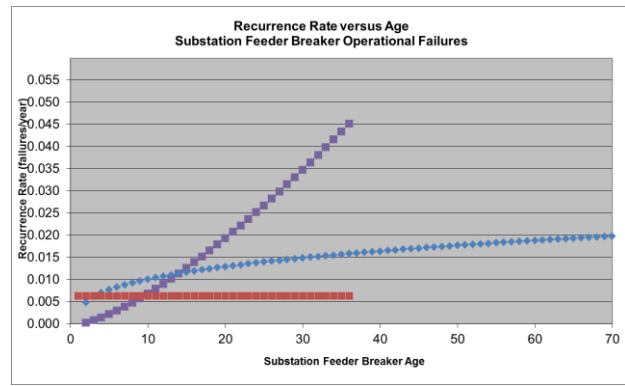


Figure 3.17 Recurrence Rates

Using these models in conjunction with the method presented in Section 2.4.2, the total expected number of operational failures in the next five years conditioned upon the current in service age of the individual breakers is 43. Oil breakers will contribute approximately 28 to the total; gas breakers are estimated to contribute approximately 12 to the total with vacuum breakers contributing the remaining 3 estimated failures. The gas breakers are disproportionally contributing to the total considering the gas breakers represent only 18% of the entire breaker fleet. Supplemental Files 4-6 provide the failure prediction calculation details.

3.2.3 Substation Component Modeling

A summary of the component reliability data used in the analysis is provided in Table 3.4.

Table 3.4 Substation Component Modeling

Component	λ (f/yr)	λ^a (f/yr)	λ_c (f/yr)	r (hrs)	s (hrs)	P_c
T-Line Feed 1	0.0201	0.0201	0.0016347	9	3.5	-
T-Line Feed 2	0.03647	0.03647	0.0016347	9	3.5	-
Xfmr 1, 2	0.03	0.03	-	70	3.5	-
H.V. Breaker 8	0.017	0.0017	-	32	3.5	0.05
L.V. Breaker 1,2,3,4,5,6,7	0.017	0.0017	-	32	3.5	0.05
Feeder 1	0.1678	0.1678	-			
Feeder 2	0.1061	0.1061	-			
Feeder 3	0.1813	0.1813	-			
Feeder 4	0.1791	0.1791	-			

The transmission line data uses line length data from Table 3.1 and component data information from Table 3.2. The transformer values are assumed. The total feeder breaker failure rate assumes that the median aged oil interrupting breaker is used. The active failure rate is taken as a tenth of the total failure rate as it was noted that 90% of the time the failure type is passive. Breaker repair time is taken from Chowdhury & Koval (2009) which is the sum of callout, isolation and repair/replace times. The high side breaker is assumed to behave similar to the feeder circuit breaker. Substation switching times are assumed. It is assumed that the busbars and disconnect switches are perfectly reliable.

Feeder failure rates are calculated as the sum of the products of the individual line lengths and respective component failure rates. The details of both the lengths and failure data are provide in Section 3.3.

3.2.4 Substation Reliability Evaluation

As was discussed in Section 2.5 the transmission and substation systems will decompose into an equivalent block in series. To do this, an equivalent source per feeder is modeled whereby all of the transmission and substation system surrounding the respective feeder breaker are reduced to an equivalent block with an expected failure rate and annual outage duration. This block will then be placed in series with its feeder in the next section and reliability indices calculated for each load point. Using the above ideas, the component data in Table 3.4, and the respective minimum cut sets results in the following equivalent source per feeder as shown in Tables 3.5 thru 3.8

Table 3.5 Feeder #1 Equivalent Source

Event	λ (f/yr)	r (hrs)	U (hrs/yr)
T. Line Feed 1 + T. Line Feed 2	0.001636206	4.5	0.0073629
T. Line Feed 1 + H.V. Breaker 8	1.59928E-06	7.0243902	1.123E-05
Xfmr 1	0.03	3.5	0.105
L.V. Breaker 5	0.017	3.5	0.0595
T. Line Feed 1A	0.0201	3.5	0.07035
H.V. Breaker 8A	0.0017	3.5	0.00595
T. Line Feed 2A + H.V. Breaker 8S	0.0018235	3.5	0.0063823
Xfmr 2A + T. Line Feed 1	8.60445E-07	2.52	2.168E-06
T. Line Feed 2A + H.V. Breaker 8S	0.0015	3.5	0.00525
L.V. Breaker 6A + T. Line Feed 1	4.87586E-08	2.52	1.229E-07
Sectionalizing Breaker 7A	0.0017	3.5	0.00595
FB2A + L.V. Breaker 6S + T. Line Feed 1	2.43793E-09	3.5	8.533E-09
FB3A + L.V. Breaker 6S + T. Line Feed 1	2.43793E-09	3.5	8.533E-09
FB4A	0.0017	3.5	0.00595
Feeder 4 + FB4S	0.0089525	3.5	0.0313338
Total (Feeder 1)	0.08611472	3.5190554	0.3030425

Table 3.6 Feeder #2 Equivalent Source

Event	λ (f/yr)	r (hrs)	U (hrs/yr)
T. Line Feed 1 + T. Line Feed 2	0.001636206	4.5	0.0073629
T. Line Feed 1 + H.V. Breaker 8	1.59928E-06	7.0243902	1.123E-05
Xfmr 1	0.03	3.5	0.105
L.V. Breaker 5	0.017	3.5	0.0595
T. Line Feed 1A	0.0201	3.5	0.07035
H.V. Breaker 8A	0.0017	3.5	0.00595
T. Line Feed 2A + H.V. Breaker 8S	0.0018235	3.5	0.0063823
Xfmr 2A + T. Line Feed 1	8.60445E-07	2.52	2.168E-06
Xfmr 2A + H.V. Breaker 8S	0.0015	3.5	0.00525
L.V. Breaker 6A + T. Line Feed 1	4.87586E-08	2.52	1.229E-07
Sectionalizing Breaker 7A	0.0017	3.5	0.00595
FB2A + L.V. Breaker 6S + T. Line Feed 1	2.43793E-09	3.5	8.533E-09
FB3A + L.V. Breaker 6S + T. Line Feed 1	2.43793E-09	3.5	8.533E-09
FB1A	0.0017	3.5	0.00595
Feeder 1 + FB1S	0.00839	3.5	0.029365
Total (Feeder 2)	0.08555222	3.5191807	0.3010737

Table 3.7 Feeder #3 Equivalent Source

Event	λ (f/yr)	r (hrs)	U (hrs/yr)
T. Line Feed 2 + T. Line Feed 1	0.001636206	4.5	0.0073629
T. Line Feed 2 + H.V. Breaker 8	2.90178E-06	7.0243902	2.038E-05
Xfmr 2	0.03	3.5	0.105
L.V. Breaker 6	0.017	3.5	0.0595
T. Line Feed 2A	0.03647	3.5	0.127645
H.V. Breaker 8A	0.0017	3.5	0.00595
T. Line Feed 1A + H.V. Breaker 8S	0.001005	3.5	0.0035175
Xfmr 1A + T. Line Feed 2	1.56122E-06	2.52	3.934E-06
Xfmr 1A + H.V. Breaker 8S	0.0015	3.5	0.00525
L.V. Breaker 5A + T. Line Feed 2	8.84689E-08	2.52	2.229E-07
Sectionalizing Breaker 7A	0.0017	3.5	0.00595
FB1A + L.V. Breaker 5S + T. Line Feed 2	4.42344E-09	3.5	1.548E-08
FB4A + L.V. Breaker 5S + T. Line Feed 2	4.42344E-09	3.5	1.548E-08
FB3A	0.0017	3.5	0.00595
Feeder 3 + FB3S	0.0090625	3.5	0.0317188
Total (Feeder 3)	0.101778267	3.5161608	0.3578687

Table 3.8 Feeder #4 Equivalent Source

Event	λ (f/yr)	r (hrs)	U (hrs/yr)
T. Line Feed 2 + T. Line Feed 1	0.001636206	4.5	0.0073629
T. Line Feed 2 + H.V. Breaker 8	2.90178E-06	7.0243902	2.038E-05
Xfmr 2	0.03	3.5	0.105
L.V. Breaker 6	0.017	3.5	0.0595
T. Line Feed 2A	0.03647	3.5	0.127645
H.V. Breaker 8A	0.0017	3.5	0.00595
T. Line Feed 1A + H.V. Breaker 8S	0.001005	3.5	0.0035175
Xfmr 1A + T. Line Feed 2	1.56122E-06	2.52	3.934E-06
Xfmr 1A + H.V. Breaker 8S	0.0015	3.5	0.00525
L.V. Breaker 5A + T. Line Feed 2	8.84689E-08	2.52	2.229E-07
Sectionalizing Breaker 7A	0.0017	3.5	0.00595
FB1A + L.V. Breaker 5S + T. Line Feed 2	4.42344E-09	3.5	1.548E-08
FB4A + L.V. Breaker 5S + T. Line Feed 2	4.42344E-09	3.5	1.548E-08
FB2A	0.0017	3.5	0.00595
Feeder 2 + FB2S	0.005305	3.5	0.0185675
Total (Feeder 4)	0.098020767	3.5167803	0.3447175

These results show that the expected unavailability at the source side of the respective feeder breaker is around 0.30 to 0.35 hours per year (roughly 18-21 minutes) as a result of the substation and transmission system failures. The distribution system contribution to this total will be calculated in the next section.

3.2.5 Distribution Reliability Assessment

The distribution system, as modified from Allan et al. (1991), is shown in Figure 3.18. The 3- \emptyset feeders getaway from the substation underground as denoted by the dotted lines and then rise up overhead. Fused taps lateral off of the backbone feeder with lengths shown in Table 3.9 feeding customers at load points as described in Table 3.10. Normally closed (NC) sectionalizing switches allow for feeder section isolation.

Normally open (NO) tie switches allow for load transfer between adjacent feeders. It is assumed that the probability of successful switching is unity for the first sectionalizing switch behind the open point then decrementing by 10% for each successive switch behind the tie switch as shown. Component failure rate and switching times, based on published literature, are assembled by Chowdhury & Koval (2009), modified slightly, and presented in Table 3.11. The repair times are the sum of the times to callout, isolate and repair.

Table 3.9 Distribution Section Lengths

Length (mi)	Sections
0.375	2, 6, 10, 12, 17, 21, 25, 28, 30, 34
0.46	4, 7, 9, 12G, 16G, 19, 22, 24, 27, 29, 32, 35
0.5	1G, 3, 5, 8, 11, 13, 14, 15, 16, 18, 20, 23, 26, 26G, 31, 33, 36, 37

Table 3.10 Load Point Customer Information

Load Points	# of Customers	Customer Type
1, 2, 3, 10, 11	210	Residential
12, 17, 18, 19	200	Residential
6, 7, 15, 16, 22	10	Small C&I
4, 5, 8, 9, 13, 14, 20, 21	1	Small C&I

Table 3.11 Distribution Component Data

Component	λ (f/yr or f/mi-yr)	r (hrs)	s (hrs)
3-Ph OH	0.09	4	1.5
1-Ph OH	0.03	3	1.5
Xfmr 3-Ph	0.03	6.5	1
Xfmr 1-Ph	0.01	3.5	1
3-Ph UG (XLPE)	0.035	24	3.5
1-Ph UG (XLPE)	0.02	11	3.5
Switch (Manual)	0.001	5.5	2
Fuse	0.003	2	1.5

The calculations will be performed using the information in the Tables above as in Section 2.5 using the equivalent source as calculated in Section 3.2.4 in the next section.

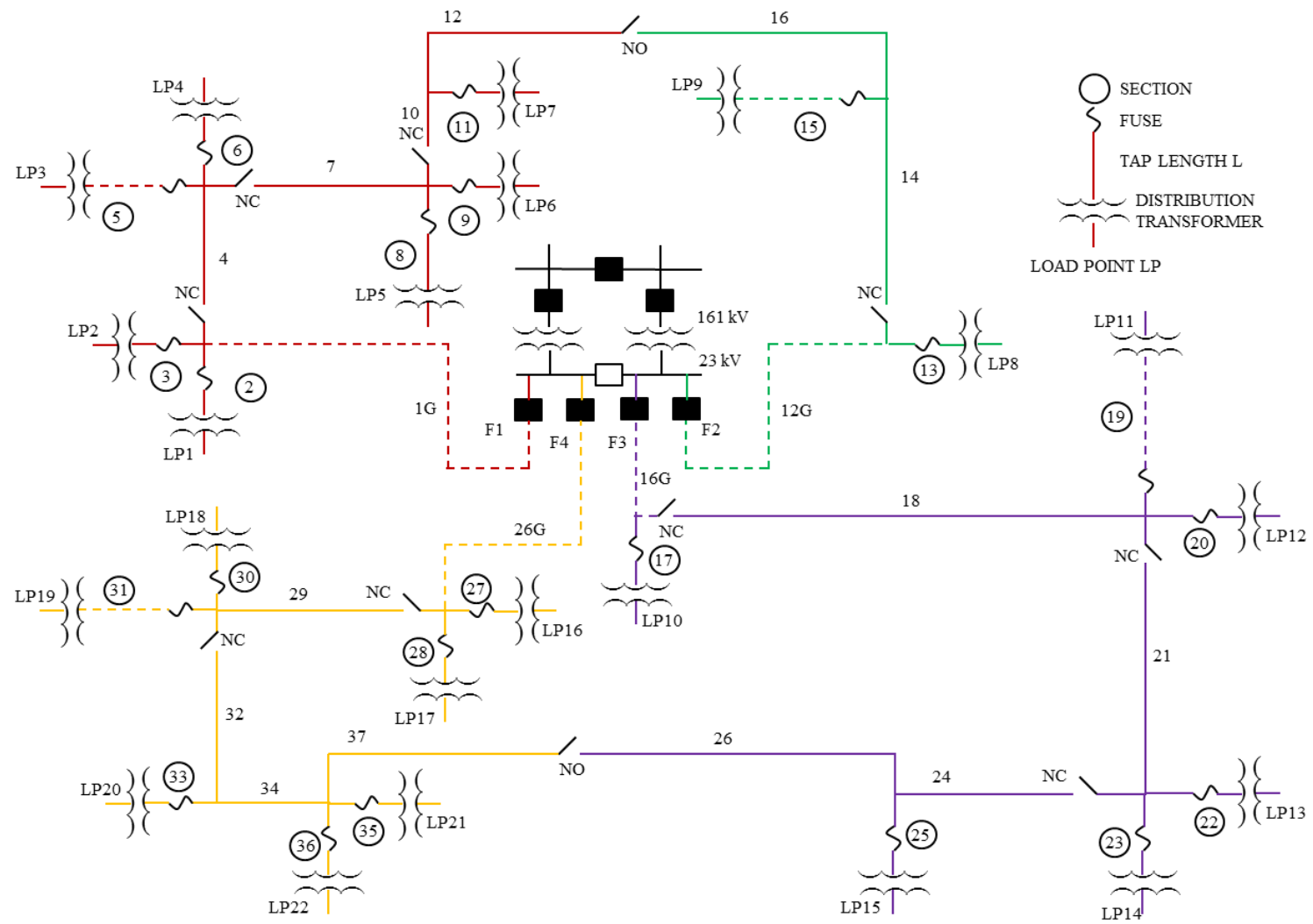


Figure 3.18 Distribution System

3.3 Composite Reliability Evaluation

The equivalent feeder source as calculated in 3.2.4 is placed in series with the respective feeder as described in Section 3.2.5. Series system calculations can then be performed as in Section 2.5. For each load point the expected failure rate, outage duration, and annual outage duration is calculated as shown in Table 3.12.

Table 3.12 Load Point Reliability Results

Feeder	Load Point	λ (f/yr)	r (hrs)	U (hrs/yr)
1	1	0.2986	3.9122	1.1684
1	2	0.3024	3.9009	1.1796
1	3	0.2974	2.8876	0.8588
1	4	0.3411	3.1744	1.0827
1	5	0.3523	2.9582	1.0421
1	6	0.3487	3.0578	1.0663
1	7	0.3224	2.8949	0.9333
2	8	0.2877	4.5657	1.3136
2	9	0.2603	4.8986	1.2750
3	10	0.3277	3.7203	1.2192
3	11	0.3257	2.9261	0.9529
3	12	0.3315	2.7054	0.8967
3	13	0.3778	2.9359	1.1091
3	14	0.3814	2.9460	1.1235
3	15	0.3701	3.0234	1.1191
4	16	0.3720	4.0983	1.5244
4	17	0.3219	3.8295	1.2327
4	18	0.3219	2.7079	0.8717
4	19	0.3207	2.9562	0.9479
4	20	0.3756	3.0061	1.1290
4	21	0.3720	3.0184	1.1227
4	22	0.3756	3.0278	1.1371

Table 3.12 shows that after adding the distribution system, the load point unavailability values increase to about 0.9 to 1.3 hrs/yr. Recall that the equivalent source unavailability values ranged from 0.3 to 0.35 hrs/yr. This implies that the distribution system accounts for roughly 70% of the total load point unavailability with the

transmission and substation representing the remaining 30% for this system. This result is fairly consistent with the 20% estimate of Billinton & Jonnavitihula (1996) as the substation contribution to load point unavailability. It also implies that assuming a perfectly reliable substation and transmission source when focusing on distribution system analysis, as is frequently done, can lead to overly optimistic results. The load point results given in Table 3.12 combined with the customer data given in Table 3.10 allow for the calculation of the reliability indices as shown in Table 3.13.

Table 3.13 Base Case Reliability Results

Feeder	CMI (mins/yr)	SAIDI (hrs/yr)	ECOST (\$/yr)
F1	54078.089	1.036	\$31,118
F2	155.317	1.294	\$2,158
F3	38934.494	1.027	\$13,893
F4	38360.215	1.028	\$27,007
System	131528.114	1.031	\$74,177

CMI is the sum of all annual customer outage minutes of interruption expected. Feeder #1 has the highest CMI as it has the most customers; conversely Feeder #2 has the lowest CMI as it has the fewest customers. Similarly, the expected SAIDI value is calculated at the feeder and system level reflecting what an average customer can expect in terms of annual outage duration. The ECOST value is the expected annual total customer outage costs. This value takes into account the customer type (residential/commercial) and the associated CDF as described in Section 2.1.2 along with the expected load point unavailabilities. It is assumed that all of the commercial customers are small C&I and all outages take place on a summer weekday. The ECOST value is strictly the expected customer outage costs; it does not include the repair costs or other associated costs to the utility.

CHAPTER 4

BUDGET-CONSTRAINED POWER SYSTEM RELIABILITY OPTIMIZATION

The modeling concepts introduced in previous sections allow for the comparison of the effects of various project options. This section will introduce multiple projects in the form of case studies. The projects are chosen from different portions of the power system (transmission, substation, distribution) to compare the impacts of potential projects from seemingly disparate work areas.

4.1 Case Studies and Evaluation

4.1.1 Base Case

The base case consists of the system and components introduced in the previous section. The reliability results of the base case were shown in Table 3.13. This case assumes that all switching is performed manually.

4.1.2 Case 1: Install Automated Switches by Feeder

One of the technologies that generally fall under the smart grid umbrella is distribution automation. Distribution automation can mean different things, ranging from a SCADA operator being able to remotely operate distribution switches to a self-healing system whereby the devices constantly poll each other and operate relatively autonomously. In this case, it is assumed that the switches are able to be remotely operated by a SCADA operator in 5 minutes as shown in Table 4.1. In the event of a fault, the operator will remotely be able to poll the devices to determine where the fault generally is located and isolate. A crew or troubleshooter is then dispatched to make the appropriate repairs. The failure rate and the repair time are taken as before from Chowdhury & Koval (2009); the manual and automated switches are assumed to be equivalent in these respects. The remaining components and assumptions are consistent with the base case.

Table 4.1 Switching Component Information

Component	λ (f/yr)	r (hrs)	s (hrs)
Switch (Manual)	0.001	5.5	2
Switch (Automated)	0.001	5.5	0.0833

The reliability results using the automated switches are presented by feeder in Table 4.2. The results assume no interaction between feeders; i.e., even though the automation of a tie switch improves the reliability of the adjacent feeder, these improvements will be ignored.

Table 4.2 Case 1 Reliability Results

Feeder	CMI (mins/yr)	SAIDI (hrs/yr)	ECOST (\$/yr)
F1	36331.068	0.696	\$22,797
F2	132.666	1.106	\$1,894
F3	23763.513	0.627	\$10,274
F4	23623.859	0.633	\$21,208

These results will be compared with the base case and discussed in Section 4.2.1 along with a calculation of the project benefit-costs.

4.1.3 Case 2: Replace Feeder Breakers by Feeder

Case 2 presents a substation project whereby an existing oil-interrupting breaker is replaced by a better performing vacuum-interrupting breaker. The feeder breaker component information is presented in Table 4.3. As before, it is assumed that the active failure rate is a tenth of the total failure rate. All other component data and assumptions are consistent with the base case.

Table 4.3 Feeder Breaker Component Information

Component	λ (f/yr)
Feeder Breaker (Oil)	0.017
Feeder Breaker (Vacuum)	0.0063

The reliability results of replacing the feeder breakers are presented by feeder in Table 4.4. These results will be compared with the base case and discussed in Section 4.2.2. along with a calculation of the project benefit-costs

Table 4.4 Case 2 Reliability Results

Feeder	CMI (mins/yr)	SAIDI (hrs/yr)	ECOST (\$/yr)
F1	52822.337	1.012	\$30,355
F2	151.69	1.264	\$2,101
F3	37732.329	0.995	\$13,546
F4	37282.2	0.999	\$26,365

4.1.4 Case 3: Replace 3-Ø Underground Getaway Cable by Feeder

The test distribution system as shown in Figure 3.18, as well as in most substations, has underground feeder getaway cables from the substation. Depending upon the cable insulation, the performance of the getaway cable can vary widely. For example, early high molecular weight polyethylene (HMWPE) insulated cables were found to be particularly susceptible to water-treeing and early failure (Thue, 1999). In the base case, the getaways are assumed to be cross-linked polyethylene (XLPE) insulated with properties listed in Table 4.5, again from Chowdhury & Koval (2009). As a representative cable retrofit example, this case assumes that the existing XLPE-insulated cables are replaced with tree-retardant cross-linked polyethylene (TRXLPE) insulated cables with properties given in Table 4.5.

Generally, an underground cable fault has a much longer repair time than an overhead line. This is due to the extended time to locate the fault, pull the faulted cable

section out of the duct system, install new cable and splice with the existing cables in the manhole or terminate appropriately.

Table 4.5 3-Ø Getaway Cable Component Information

Component	λ (f/mi-yr)	r (hrs)
3-Ph UG (XLPE)	0.035	24
3-Ph UG (TRXLPE)	0.028	24

The reliability results of replacing the feeder getaways are presented by feeder in Table 4.6. These results will be compared with the base case and discussed in Section 4.2.3 along with a calculation of the project benefit-costs.

Table 4.6 Case 3 Reliability Results

Feeder	CMI (mins/yr)	SAIDI (hrs/yr)	ECOST (\$/yr)
F1	51538.779	0.987	\$30,664
F2	144.768	1.206	\$2,029
F3	37431.878	0.987	\$13,759
F4	36742.492	0.985	\$26,248

4.1.5 Case 4: Replace 1-Ø Underground Residential Distribution Cable by Feeder

The same issues described in the previous section apply to 1-Ø cables typically feeding residential neighborhoods. Some of these neighborhoods can have cable that is direct-buried instead of conduited. This makes the fault location and repair times significantly longer than a conduited system. These direct-buried cables can also have a higher failure rate due to environmental exposure. This case study will not directly address direct-buried cables other than to note the differences in installation. As a representative URD installation, this case study examines the replacement of the 1-Ø cables that feed the associated underground taps in the test distribution as shown in

Figure 3.18. It is assumed again that the existing XLPE-insulated cables will be replaced with better performing TRXLPE-insulated cables, both with properties shown in Table 4.7 (Chowdhury & Koval, 2009).

Table 4.7 1-Ø URD Cable Component Information

Component	λ (f/mi-yr)	r (hrs)
1-Ph UG (XLPE)	0.02	11
1-Ph UG (TRXLPE)	0.013	11

The reliability results of replacing the 1-Ø URD cables are presented by feeder in Table 4.8. These results will be compared with the base case and discussed in Section 4.2.4 along with a calculation of the project benefit-costs.

Table 4.8 Case 4 Reliability Results

Feeder	CMI (mins/yr)	SAIDI (hrs/yr)	ECOST (\$/yr)
F1	53592.157	1.027	\$31,104
F2	155.317	1.294	\$2,158
F3	38487.712	1.015	\$13,881
F4	37897.683	1.015	\$26,994

4.1.6 Case 5: 161 kV Transmission Improvements

As was shown in Figure 3.1, both transmission feeds to the substation share a common-tower for an extended portion of the route. This common-tower arrangement makes these feeds susceptible to common-cause failures such as vehicle impacts, etc. In Case 5, an alternate route is planned whereby additional structures are added and adjacent transmission circuits are reconfigured to reduce the common-tower exposure. The proposed arrangement is shown in Figure 4.1. As shown in Table 4.9, the common-tower arrangement exposure is reduced from 8,627' to 750'; the total length of feed #2 is also reduced.

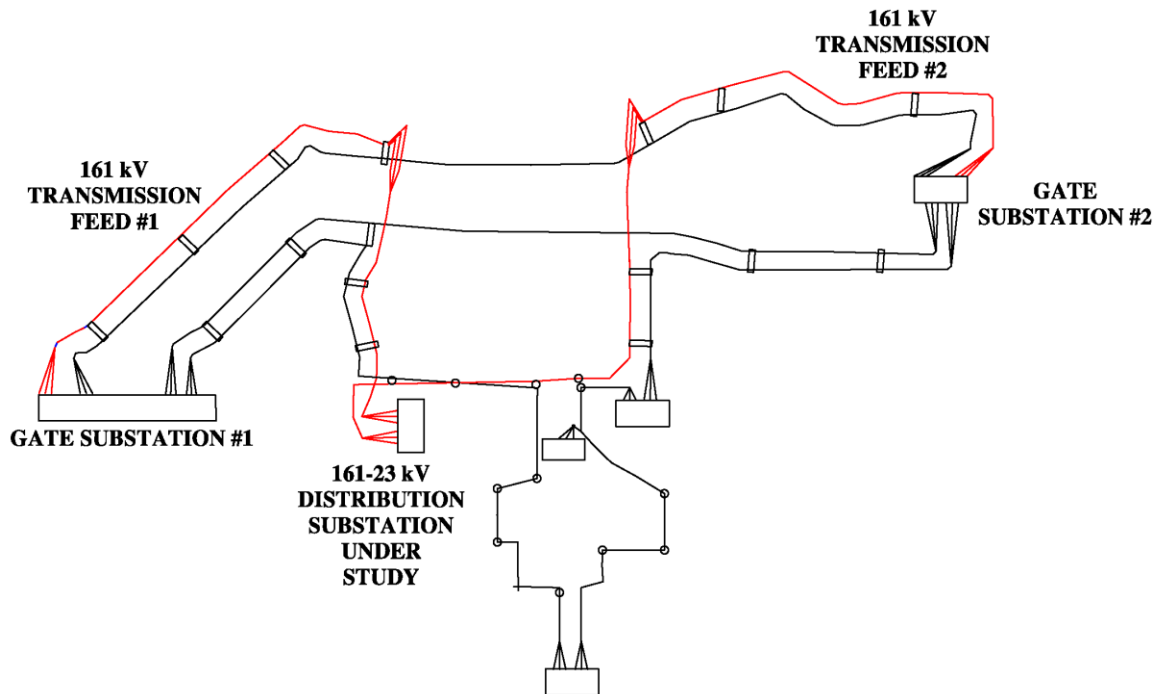


Figure 4.1 Proposed Transmission Improvements

Table 4.9 Proposed Transmission Circuit Lengths

Circuit	Existing/Proposed	Length (ft)
Feed #1	Existing	21,265
Feed #2	Existing	37,517
Common-Tower	Existing	8,627
Feed #1	Proposed	21,265
Feed #2	Proposed	35,465
Common-Tower	Proposed	750

Applying the model shown in Figure 2.7 with the outage data in Section 3.1 results in the steady-state probability of being in State 4 (both circuits down) shown in Figure 4.2 for various values of λ_c/λ for both the existing and proposed cases.

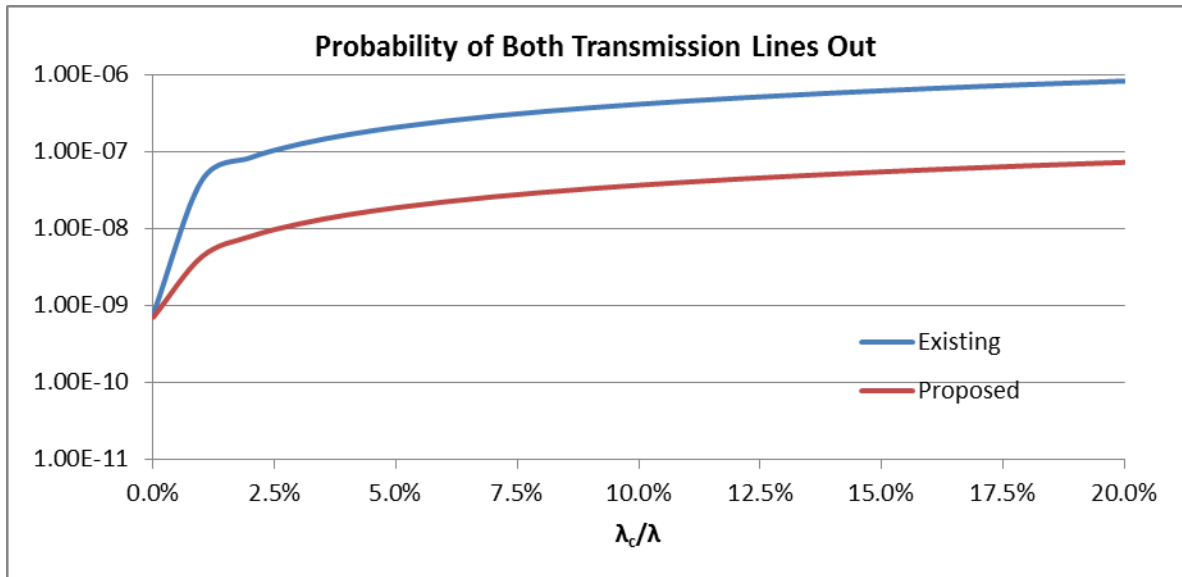


Figure 4.2 State 4 Probabilities for Transmission Lines

At $\lambda_c/\lambda = 20\%$, the steady-state probability of both lines down for the existing case is 8.3686×10^{-7} ; for the proposed case the steady-state probability of both lines down is 7.3552×10^{-8} – a 91% reduction. These values can be interpreted as the proportion of time these arrangements are expected to spend in these states. Since the lines are in a parallel arrangement, we can sum the steady-state probabilities of States 1, 2

& 3 to find that we expect to find the lines up 99.9999163% of the time for the existing case and 99.999993% of the time for the proposed case. The reliability results of the transmission system improvements are presented in Table 4.10.

Table 4.10 Case 5 Reliability Results

Feeder	CMI (mins/yr)	SAIDI (hrs/yr)	ECOST (\$/yr)
F1	53796.875	1.031	\$30,996
F2	154.664	1.289	\$2,148
F3	38460.710	1.014	\$13,763
F4	37892.706	1.015	\$26,733
System	130304.955	1.022	\$73,640

These results will be compared with the base case and discussed in Section 4.2.5 along with a calculation of the project benefit-costs.

4.2 Budget-Constrained Project Optimization

4.2.1 Case 1 (Install Automated Switches) Reliability Benefit-Cost Analysis

Installing automated switches results in the expected changes as shown in Table 4.11 for each of the respective feeders. It is obvious from the results that the greatest CMI impact is at Feeder #1, whereas the greatest SAIDI impact is at Feeder #3. The difference is that as Feeder #1 has more customers than Feeder #3 the SAIDI numerator is larger for Feeder #1 and the SAIDI denominator is smaller for Feeder #3. The greatest reduction in customer-outage costs is at Feeder #1, again as a result of the large number of customers.

It is interesting to note that this project option does not change the failure rate at any of the load points as none of the component failure rates changed. The only thing that changed was the response time. This is interesting in that it could effectively change the operating philosophy from prioritizing retrofits of equipment to improving the response and flexibility to failures. This is important as the distribution systems are spatially very large with varying types of equipment placed in service at different times;

data available for component modeling at many utilities is sparse to non-existent. The managed response via improved isolation times via automated switching is a very clean solution to this type of problem. The project costs are based upon estimates by the utility based upon historical installation costs.

Table 4.11 Case 1 Reliability Improvements & Project Costs

Feeder	Δ_{CMI}	Δ_{SAIDI}	Δ_{ECOST}	# Switches	Cost/Switch
F1	17747.020	0.340	\$8,321	4	\$60,000
F2	22.650	0.189	\$263	2	\$60,000
F3	15170.981	0.400	\$3,619	4	\$60,000
F4	14736.355	0.395	\$5,800	4	\$60,000

Table 4.12 presents the reliability benefit-costs of the project at the feeders. The BCA_{CMI} value is simply the project costs divided by the change in CMI. This value can be thought of as the dollars spent per customer-minute of interruption avoided. These are then ranked relative to each other by feeder. This is done similarly for SAIDI and the customer outage costs. These comparisons are done to see how the differing comparison methodologies will ultimately rank projects. It should be noted that the BCA for the customer outage costs, even though measured in dollars, doesn't imply that a value of 1 means the benefit dollars equal the project costs; the unity value simply means that it is the best project and others are compared to it in decreasing value.

Table 4.12 Case 1 Reliability Benefit-Cost Analysis

Feeder	BCA_{CMI} (\$/CMI)	Relative BCA_{CMI}	$\text{BCA}_{\text{SAIDI}}$ (\$/hr)	Relative $\text{BCA}_{\text{SAIDI}}$	$\text{BCA}_{\text{ECOST}}$	Relative $\text{BCA}_{\text{ECOST}}$
F1	\$13.52	1.000	\$705,921	1.177	0.035	1.000
F2	\$5,297.90	391.758	\$635,748	1.060	0.002	0.063
F3	\$15.82	1.170	\$599,882	1.000	0.015	0.435
F4	\$16.29	1.204	\$607,803	1.013	0.024	0.697

4.2.2 Case 2 (Feeder Breaker Replacement) Reliability Benefit-Cost Analysis

Replacing oil breakers with better performing vacuum breakers results in the following changes as shown in Figure 4.13. Here again the Feeder #1 CMI results are better than Feeder #3 whereas the Feeder #3 SAIDI results are better than Feeder #1 strictly as a result of the difference in customers between feeders reflected in the SAIDI calculation. The project costs are estimated by the utility Substation Engineering department based upon historical replacement costs.

Table 4.13 Case 2 Reliability Improvements & Project Costs

Feeder	Δ_{CMI}	Δ_{SAIDI}	Δ_{ECOST}	Cost/Breaker
F1	1255.752	0.024	\$763	\$125,000
F2	3.627	0.030	\$57	\$125,000
F3	1202.165	0.032	\$347	\$125,000
F4	1078.015	0.029	\$642	\$125,000

The BCA values and relative rankings are presented in Table 4.14. It is already obvious that the BCA_{CMI} as measured by \$/CMI spent is much higher for this project than for automating switches; more on this in Section 4.2.6. The low number of customers on Feeder #2 makes this an unattractive option as shown by the high BCA_{CMI} value.

Table 4.14 Case 2 Reliability Benefit-Cost Analysis

Feeder	BCA_{CMI} (\$/CMI)	Relative BCA_{CMI}	BCA_{SAIDI} (\$/hr)	Relative BCA_{SAIDI}	BCA_{ECOST}	Relative BCA_{ECOST}
F1	\$100	1.000	\$5,212,958	1.324	6.108E-03	1.000
F2	\$34,464	346.231	\$4,124,367	1.048	4.524E-04	0.074
F3	\$104	1.045	\$3,936,571	1.000	2.779E-03	0.455
F4	\$116	1.165	\$4,329,327	1.100	5.139E-03	0.841

4.2.3 Case 3 (3-Ø Getaway Cable Replacement) Reliability Benefit-Cost Analysis

The reliability results for replacing the XLPE-insulated 3-Ø underground feeder getaway cables with TRXLPE-insulated cables are shown in Table 4.15. The project costs assume that the material costs are \$100/circuit foot and that material costs represent 80% of the total project costs. Cable material costs depend on metals pricing; this value is reasonable given utility historical experience. The total cost per circuit foot installed is therefore \$125/foot.

Table 4.15 Case 3 Reliability Improvements & Project Costs

Feeder	Δ_{CMI}	Δ_{SAIDI}	Δ_{ECOST}	Project Cost
F1	2539.310	0.049	\$454	\$330,000
F2	10.549	0.088	\$128	\$303,600
F3	1502.616	0.040	\$134	\$303,600
F4	1617.723	0.043	\$759	\$330,000

The BCA values and relative ranking are provided in Table 4.16. Here Feeder #1 is the most attractive replacement option based on CMI, whereas feeder #4 would take priority based upon minimizing customer-outage costs. Feeder #2 is an unattractive option for either case due to the small number of customers.

Table 4.16 Case 3 Reliability Benefit-Cost Analysis

Feeder	BCA_{CMI} (\$/CMI)	Relative BCA_{CMI}	BCA_{SAIDI} (\$/hr)	Relative BCA_{SAIDI}	BCA_{ECOST}	Relative BCA_{ECOST}
F1	\$130	1.000	\$6,783,734	1.964	1.377E-03	0.599
F2	\$28,780	221.462	\$3,453,655	1.000	4.219E-04	0.183
F3	\$202	1.555	\$7,661,647	2.218	4.430E-04	0.193
F4	\$204	1.570	\$7,612,925	2.204	2.300E-03	1.000

4.2.4 Case 4 (1-Ø URD Cable Replacement) Reliability Benefit-Cost Analysis

The reliability results for replacing the XLPE-insulated 1-Ø URD cables with TRXLPE-insulated cables are shown in Table 4.17. The project costs assume that the material costs are a third of the 3-Ø installed costs, or \$41.67/ft. This is reasonable based upon the historical experience for the utility. There are no customers on Feeder #2 fed from a 1-Ø source.

Table 4.17 Case 4 Reliability Improvements & Project Costs

Feeder	Δ_{CMI}	Δ_{SAIDI}	Δ_{ECOST}	Project Cost
F1	485.932	0.009	\$14	\$110,000
F3	446.781	0.012	\$13	\$101,200
F4	462.532	0.012	\$14	\$110,000

The BCA values and relative ranking are provided in Table 4.18. Here Feeder #1 & Feeder #3 are essentially a toss-up as to which would be prioritized based upon CMI.

Table 4.18 Case 4 Reliability Benefit-Cost Analysis

Feeder	BCA_{CMI} (\$/CMI)	Relative BCA_{CMI}	BCA_{SAIDI} (\$/hr)	Relative BCA_{SAIDI}	BCA_{ECOST}	Relative BCA_{ECOST}
F1	\$226	1.000	\$11,816,478	3.421	1.302E-04	1.000
F3	\$227	1.001	\$8,589,225	2.487	1.267E-04	0.973
F4	\$238	1.051	\$8,875,499	2.570	1.228E-04	0.943

4.2.5 Case 5 Reliability Benefit-Cost Analysis

The reliability results for the proposed 161 kV transmission improvements to reduce the common-cause failure mode exposure are provided in Table 4.19 for the entire system. The project cost estimate of \$6,000,000 was prepared by the Substation & Transmission Engineering department of the utility.

Table 4.19 Case 5 Reliability Improvements

Feeder	Δ_{CMI}	Δ_{SAIDI}	Δ_{ECOST}	Project Cost
System	1223.159	0.010	\$537	\$6,000,000

The BCA value for the entire system is provided in Table 4.20. There is no feeder comparison as the transmission feeds essentially affect all feeders. It is obvious, however, that spending \$4,905 per CMI avoided is much higher than the \$13.52 spent for automating the switches on Feeder #1.

Table 4.20 Case 5 Reliability Benefit-Cost Analysis

Feeder	BCA_{CMI} (\$/CMI)	$\text{BCA}_{\text{SAIDI}}$ (\$/hr)	$\text{BCA}_{\text{ECOST}}$
System	\$4,905	\$625,724,009	\$11,167

4.2.6 Budget Constrained Reliability Optimization

The changes in expected reliability and associated benefit-cost analyses were quantified for all of the project options in previous sections. These can now be assembled and ranked according to increasing dollars spent per CMI purchased as shown in Table 4.21. As seen, the most cost-effective option is to automate the switches on Feeder #1 with Feeder #3 and Feeder #4 following thereafter. A utility with a constrained budget would spend budget dollars in this order to maximize the reliability benefit. It should be noted that the benefits and associated rankings could change if some project (or set of projects) is completed.

Table 4.21 CMI-Optimized Global Solution For Power System

Project	Line	Δ_{CMI}	Project Cost	BCA_{CMI} (\$/CMI)	Relative BCA_{CMI}
Install Automated Switches	F1	17747.020	\$240,000	\$13.52	1.000
Install Automated Switches	F3	15170.981	\$240,000	\$15.82	1.170
Install Automated Switches	F4	14736.355	\$240,000	\$16.29	1.204
Replace Feeder Breaker	F1	1255.752	\$125,000	\$99.54	7.361
Replace Feeder Breaker	F3	1202.165	\$125,000	\$103.98	7.689
Replace Feeder Breaker	F4	1078.015	\$125,000	\$115.95	8.574
Replace 3-Ø UG Getaway Cables	F1	2539.310	\$330,000	\$129.96	9.610
Replace 3-Ø UG Getaway Cables	F3	1502.616	\$303,600	\$202.05	14.941
Replace 3-Ø UG Getaway Cables	F4	1617.723	\$330,000	\$203.99	15.084
Replace 1-Ø UG URD Cables	F1	485.932	\$110,000	\$226.37	16.739
Replace 1-Ø UG URD Cables	F3	446.781	\$101,200	\$226.51	16.749
Replace 1-Ø UG URD Cables	F4	462.532	\$110,000	\$237.82	17.586
161 kV Transmission Improvements	All	1223.159	\$6,000,000	\$4,905.33	362.729
Install Automated Switches	F2	22.650	\$120,000	\$5,297.90	391.758
Replace 3-Ø UG Getaway Cables	F2	10.549	\$303,600	\$28,780.46	2128.197
Replace Feeder Breaker	F2	3.627	\$125,000	\$34,464.49	2548.508

The cumulative CMI-avoided and budget dollars spent can then be plotted without interaction as shown in Figure 4.3. It is obvious from the plot that there is a decreasing benefit per budget dollar spent. For the assembled list of project options, the total CMI benefit if all of the projects were done is 59,505 customer interruption minutes avoided at a cost of \$9,258,400. The utility can purchase, however, 47,654 customer-minutes of interruption avoided (80% of the total if all projects were completed) at a total cost of \$720,000 – roughly 8% of the total for all projects. A fixed capital budget would therefore fund all projects up to that capital budgeted value and not fund projects that are less cost-effective.

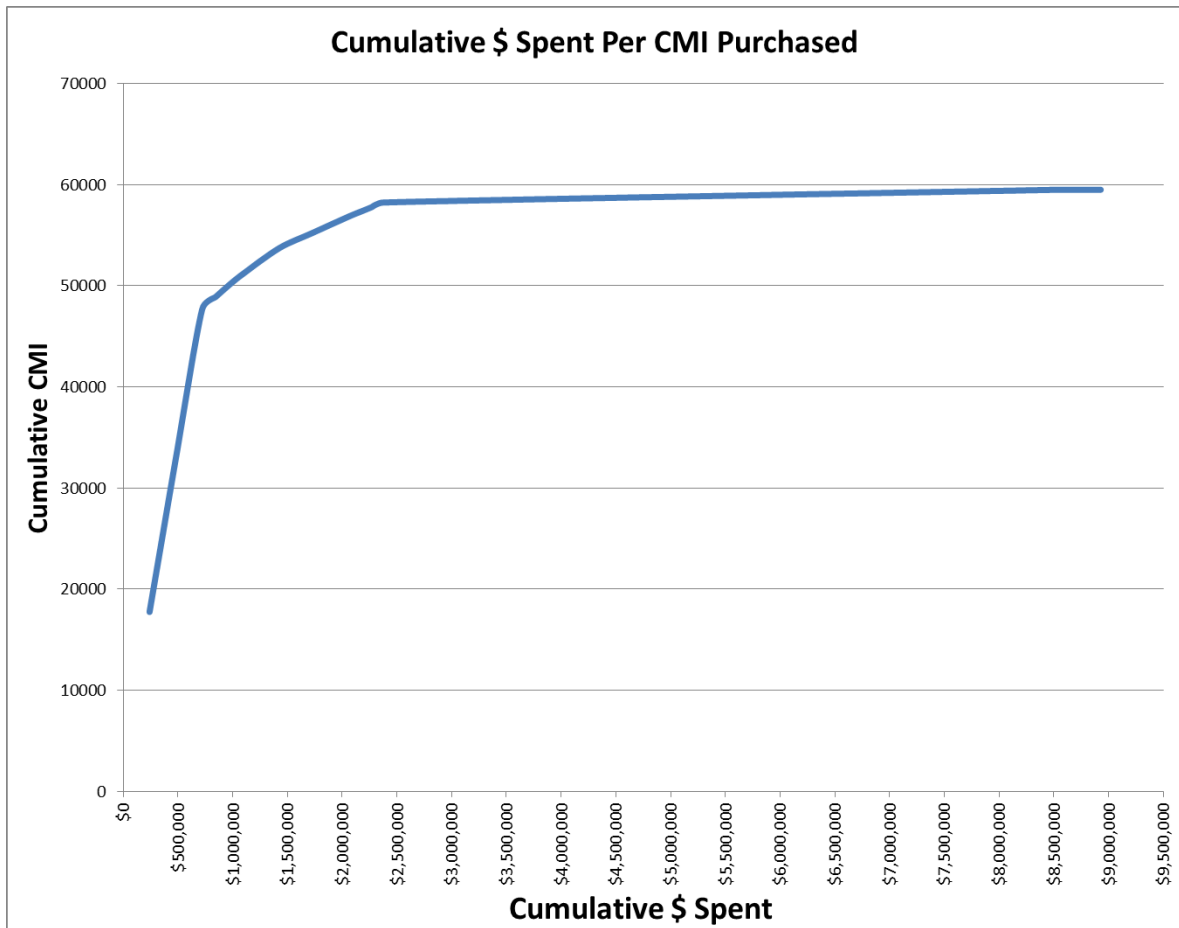


Figure 4.3 Cumulative Budget Per CMI Purchased

CHAPTER 5

CONCLUSIONS AND RECOMMENDATIONS

5.1 Conclusions

The main goal of this thesis was to provide a framework for a utility to maximize the reliability benefit for constrained budget dollars. Utility planners need ways to evaluate the impact of seemingly disparate transmission, substation, and distribution projects. Predictive reliability modeling of a hybrid transmission and substation in operation at a utility in the Southeastern United States feeding a test distribution system measured the impacts of potential projects. These impacts were defined as the change in CMI, SAIDI, and customer-outage costs. The costs associated with each project option were then used to evaluate the reliability benefit-cost. Projects were then ranked according to the budget dollars spent per customer-minute of interruption avoided. It was shown that a large portion of the total reliability improvement by doing all of the projects could be purchased by only doing a small portion of the projects. A utility could therefore choose to fund only those projects that maximize the reliability benefit.

5.2 Future Work

Future work using these ideas would include capacity constraints of the transmission, substation, and distribution systems. This was hinted at in this work in the distribution system analysis by providing a probability of successful switching. This would require a greater knowledge of the demand curves of the customers served. This will become easier as utilities embrace smart grid technologies such as smart meters and distribution automation. The effects and maintenance outages and failures overlapping maintenance outages could be performed. Weather impacts could be modeled, and the effects of various tree-trimming cycles could be evaluated as a comparison project to the ones considered here. True optimization using various crew type availability could be performed, as well as the optimal siting of automated switches.

LIST OF REFERENCES

- Aguero, J.R., Spare, J., Philips, E., O'Meally, C., Wang, J., and Brown, R.E. "Distribution System Reliability Improvement Using Predictive Models", Presented at IEEE Power and Energy Society General Meeting, 2009.
- Allan, R.N., Billinton, R., Sjarief, I., Goel, L., and So, K.S. "A Reliability Test Systems for Educational Purposes – Basic Distribution System Data and Results", IEEE Transactions on Power Systems, 1991.
- Ascher, H and Feingold, H. Repairable Systems Reliability, New York, NY, Marcel Dekker, Inc., 1984.
- Billinton, R. "Basic Models and Methodologies for Common Mode and Dependent Transmission Outage Events", Presented at IEEE Power and Energy Society General Meeting, 2012.
- Billinton, R. and Allan, R.N. *Reliability Evaluation of Engineering Systems*, 2nd Edition, New York, NY, Plenum Press, 1992.
- Billinton, R. and Allan, R.N. *Reliability Evaluation of Power Systems*, 2nd Edition, New York, NY, Plenum Press, 1996.
- Billinton, R. and Jonnavitihula, S. "A Test System for Teaching Overall Power System Reliability Assessment", IEEE Transactions on Power Systems, 1996.
- Billinton, R., Medicheria, T.K.P., and Sachdev, M.S. "Common-Cause Outages in Multiple Circuit Transmission Lines", IEEE Transactions on Reliability, 1978.
- Billinton, R., and Medicheria, T.K.P. "Station Originated Multiple Outages in the Reliability Analysis of a Composite Generation and Transmission System", IEEE Transactions on Power Apparatus and Systems, 1981.
- Brown, R.E. *Electric Power Distribution Reliability*, 2nd Edition, Boca Raton, FL, CRC Press, 2009.
- Brown, R.E. and Marshall, M.M. "Budget Constrained Planning to Optimize Power System Reliability", IEEE Transactions on Power Systems, 2000.
- Brown, R.E., and Taylor, T.M. "Modeling the Impact of Substation Distribution Reliability", IEEE Transactions on Power Systems, 1999.
- Bumblauskas, D., Meeker, W., and Gemmill, D. "Maintenance and Recurrent Event Analysis of Circuit Breaker Population Data", International Journal of Quality and Reliability Management, 2012.
- Chowdhury, A.A., and Koval, D.O. *Power Distribution System Reliability*, Hoboken, N.J., John Wiley & Sons, Inc., 2009.
- Crow, L.H. "Reliability Analysis of Complex, Repairable Systems", Technical Report 126, AMSAA, Aberdeen Proving Ground, MD, 1975.
- Ebeling, C.E. *An Introduction to Reliability and Maintainability Engineering*, 2nd Edition, Long Grove, IL, Waveland Press, Inc., 2010.
- FEMA Benefit-Cost Analysis Re-engineering (BCAR) – Risk Analysis Methodologies, Version 4.0, November 2008.
- Heising, C.R. "Reliability of Medium-Voltage Vacuum Power Circuit-Breakers", IEEE Transactions on Reliability, 1983.
- IEEE Guide for Electric Power Distribution Reliability Indices*, IEEE Standard 1366, May 2012.
- IEEE Guide for Diagnostics and Failure Investigation of Power Circuit Breakers*, IEEE Standard C37-10-2011, Dec. 2011.

- Landgren, G.L, Schneider, A.W., Bhavaraju, M.P., and Balu, N. J. “Transmission Outage Performance Prediction: Unit or Component Approach?”, IEEE Transactions on Power Systems, 1986.
- Lawton L., Sullivan M., Van Liere, K., Katz, A., and Eto, J. “A Framework and Review of Customer Outage Costs: Integration and Analysis of Electric Utility Outage Cost Surveys”. Lawrence Berkeley National Laboratory. LBNL-54365, 2003.
- Lindquist, T.M., Bertling, L., and Eriksson, R. “Circuit Breaker Failure Data and Reliability Modeling”, IET Generation, Transmission & Distribution, 2008.
- Masud, E. “Automatic Load Flow Contingency Evaluation Using a Reliability Index”, Presented at IEEE Power and Energy Society summer Meeting, 1976.
- Meeker, W.Q. and Escobar, L.A. Statistical Methods for Reliability Data, New York, NY, John Wiley & Sons, 1998.
- Nelson, W.B. *Recurrent Events Data Analysis for Product Repairs, Disease Recurrences, and Other Applications*, Philadelphia, PA, Society for Industrial and Applied Mathematics, 2003.
- Sullivan, M.J. and Keane, D.M., “Outage Cost Estimation Guidebook”, EPRI Research Project 2878-04 Final Report, December 1995.
- Task Force on Common Mode Outages of Bulk Supply Facilities of the Application of Reliability Methods Subcommittee of Power System Engineering Committee, “Common Mode Forced Outages of Overhead Transmission Lines”, IEEE Transactions on Power Apparatus and Systems, 1976.
- Thue, W.A. *Electrical Power Cable Engineering*, 2nd Edition, New York, NY, Marcel Dekker, Inc., 2003.
- Trindade, D. and Swami, N. “Statistical Analysis of Field Data for Repairable Systems”, Proc. Annual Reliability & Maintainability Symp., 2006.
- Willis, H.L. and Schrieber, R.R. *Aging Power Delivery Infrastructure*, 2nd Edition, Boca Raton, FL, CRC Press, 2013.

VITA

Jon Mosteller is a licensed professional engineer in the State of Tennessee. He received his Bachelors Degree in Civil Engineering from Christian Brothers University in 1998 with an emphasis in Environmental Engineering. Since then, he has worked in various capacities at Memphis Light, Gas & Water designing electrical substations as a substation engineer; overseeing the material testing laboratory and developing material and construction standards as a systems engineer; and currently as lead planning engineer where his responsibilities include writing the electric master plan and developing a \$70+ million electric capital budget. In his time at MLGW, he has written Pre-Disaster Mitigation grants for the seismic retrofit of power system components that ultimately have netted nearly \$3 million in awarded grant dollars.

He currently resides in Memphis with his wife, Christian, and children, Caroline & Jack.